Revision of *'Balaena' belgica* reveals a new right whale species, the possible ancestry of the northern right whale, *Eubalaena glacialis*, and the ages of divergence for the living right whale species
Please read the **Important notes** below, the **Review guidance** on page 2 and our **Standout reviewing tips** on page 3. When ready **submit online**. The manuscript starts on page 4.

Important notes

Editor and deadline

J. Thewissen / 4 Mar 2017

Files	14 Figure file(s) 2 Table file(s) 1 Other file(s) Please visit the overview page to **download and review** the files not included in this review PDF.
Declarations	**Describes a new species.**

For assistance email **peer.review@peerj.com**

Please read in full before you begin

How to review

When ready **submit your review online**. The review form is divided into 5 sections. Please consider these when composing your review:

1. **BASIC REPORTING**
2. **EXPERIMENTAL DESIGN**
3. **VALIDITY OF THE FINDINGS**
4. General comments
5. Confidential notes to the editor

You can also annotate this PDF and upload it as part of your review

To finish, enter your editorial recommendation (accept, revise or reject) and submit.

BASIC REPORTING

- Clear, unambiguous, professional English language used throughout.
- Intro & background to show context. Literature well referenced & relevant.
- Structure conforms to **PeerJ standards**, discipline norm, or improved for clarity.
- Figures are relevant, high quality, well labelled & described.
- Raw data supplied (see **PeerJ policy**).

EXPERIMENTAL DESIGN

- Original primary research within **Scope of the journal**.
- Research question well defined, relevant & meaningful. It is stated how the research fills an identified knowledge gap.
- Rigorous investigation performed to a high technical & ethical standard.
- Methods described with sufficient detail & information to replicate.

VALIDITY OF THE FINDINGS

- Impact and novelty not assessed. Negative/inconclusive results accepted. *Meaningful* replication encouraged where rationale & benefit to literature is clearly stated.
- Data is robust, statistically sound, & controlled.

- Conclusions are well stated, linked to original research question & limited to supporting results.
- Speculation is welcome, but should be identified as such.

Revision of *'Balaena' belgica* reveals a new right whale species, the possible ancestry of the northern right whale, *Eubalaena glacialis*, and the ages of divergence for the living right whale species

Michelangelo Bisconti Corresp., 1 , **Olivier Lambert** 2 , **Mark Bosselaers** 2, 3

1 San Diego Natural History Museum, San Diego, U.S.A.

2 Royal Belgian Institute of Natural Sciences, Brussels, Belgium

3 Zeeland Royal Society of Sciences, Middelburg, The Netherlands

Corresponding Author: Michelangelo Bisconti
Email address: michelangelobisconti@gmail.com

In 1941, O. Abel established *Balaena belgica* based on a series of fused cervical vertebrae and citing other cranial fragments from the late Neogene of the Antwerp harbor (northern Belgium). Later, Plisnier-Ladame and Quinet (1969) added a neurocranium and other skeletal remains from the same area to this species. Recently, the neurocranium was re-assigned to the genus *Eubalaena* thanks to newer phylogenetic analyses. Here, a new description is provided of materials previously assigned to *'Balaena' belgica* together with taxonomic revisions. Our work suggests that the cervical complex originally designated as the type of *'Balaena' belgica* is too poorly preserved to be used as such and is assigned to Balaenidae gen. et sp. indet., thus making *'Balaena' belgica* a nomen dubium. In addition to the neurocranium, the other remains consist in a fragment of maxilla assigned to Balaenidae gen. et sp. indet. and in a humerus assigned to *Eubalaena* sp. Discovered in the Kruisschans Sands Member of the Lillo Formation (3.2-2.8 Ma, Piacenzian, Late Pliocene), the neurocranium is designated as the holotype of the new species *Eubalaena ianitrix*. Our phylogenetic analysis supports a sister-group relationship of *E. ianitrix* and *E. glacialis*, and helps constraining the ages of origin for balaenid clades. Ecological and phylogenetic data suggest that *E. ianitrix* may represent the direct ancestor of *E. glacialis*, the latter having evolved through phyletic transformation including body size increase during the temperature decline of the Late Pliocene.

1 **Revision of *'Balaena' belgica* reveals a new right whale species, the possible**

2 **ancestry of the northern right whale, *Eubalaena glacialis*, and the ages of**

3 **divergence for the living right whale species**

5 Michelangelo Bisconti,[1] Olivier Lambert[2] and Mark Bosselaers[2,3]

7 [1]San Diego Natural History Museum, Balboa Park, 1788 El Prado, San Diego, CA 92101, USA

8 [2]Royal Belgian Institute of Natural Sciences, Rue Vautier 29, 1000 Brussels, Belgium

9 [3]Zeeland Royal Society of Sciences, Middelburg, The Netherlands

11 Corresponding Author

12 Michelangelo Bisconti

13 Email address: michelangelobisconti@gmail.com

ABSTRACT

In 1941, O. Abel established *Balaena belgica* based on a series of fused cervical vertebrae and citing other cranial fragments from the late Neogene of the Antwerp harbor (northern Belgium). Later, Plisnier-Ladame and Quinet (1969) added a neurocranium and other skeletal remains from the same area to this species. Recently, the neurocranium was re-assigned to the genus *Eubalaena* thanks to newer phylogenetic analyses. Here, a new description is provided of materials previously assigned to *'Balaena' belgica* together with taxonomic revisions. Our work suggests that the cervical complex originally designated as the type of *'Balaena' belgica* is too poorly preserved to be used as such and is assigned to Balaenidae gen. et sp. indet., thus making *'Balaena' belgica* a nomen dubium. In addition to the neurocranium, the other remains consist in a fragment of maxilla assigned to Balaenidae gen. et sp. indet. and in a humerus assigned to *Eubalaena* sp. Discovered in the Kruisschans Sands Member of the Lillo Formation (3.2-2.8 Ma, Piacenzian, Late Pliocene), the neurocranium is designated as the holotype of the new species *Eubalaena ianitrix*. Our phylogenetic analysis supports a sister-group relationship of *E. ianitrix* and *E. glacialis*, and helps constraining the ages of origin for balaenid clades. Ecological and phylogenetic data suggest that *E. ianitrix* may represent the direct ancestor of *E. glacialis*, the latter having evolved through phyletic transformation including body size increase during the temperature decline of the Late Pliocene.

Subjects Anatomy, Cetacea, Evolution, Phylogeny, Palaeontology, Skull, Zoology.

Keywords Cetacea, Balaenidae, *Eubalaena ianitrix*, Mysticeti, Phylogeny, Pliocene

38 **Introduction**

40 Living right whales include North Atlantic, southern and North Pacific right whales, all of them

41 grouped within the genus *Eubalaena* (Cetacea, Mysticeti, Balaenidae; Kenney, 2009; Rice, 2009).

42 The North Atlantic or northern right whale obviously inhabits the North Atlantic ocean, the

43 southern right whale is distributed in the waters around Antarctica, and the North Pacific right

44 whale is present in a portion of the Pacific that is limited in the south by southern Japan and the

45 southern portion of the California peninsula (Kenney, 2009). Recent studies have addressed

46 molecular taxonomy, population dynamics, and distribution patterns of these whales suggesting

47 that the genus *Eubalena* should include three species corresponding to the three groups mentioned

48 above (namely, *Eubalaena glacialis*, *E. australis* and *E. japonica*) (e.g., Rosenbaum et al., 2000).

49 Although a full agreement on this point has not been reached yet, it is largely acknowledged that

50 North Atlantic and North Pacific right whales are suffering high extinction risk (e.g., Clapham et

51 al., 1999). This is probably due to the catastrophic bottleneck effect induced into their populations

52 by human hunting activities during 19th and 20th centuries (e.g., Gaskin, 1986) that drastically

53 reduced the size of their populations in a brief period.

54 The assessment of the genetic diversity of the living right whale populations largely depends on

55 the reconstruction of the population size before the start of industrial whaling (Rooney et al., 2001;

56 Rosenbaum et al., 2000, Malik et al., 2000). Such a reconstruction, in its turn, depends on several

57 factors including the phylogenetic history of the genus and divergence time from the living species

58 that is phylogenetically closest to the living right whales (Rooney et al., 2001), namely the

59 bowhead whale *Balaena mysticetus*. The study of the fossil record may help determining the

60 antiquity of the genus *Eubalaena* and constraining the time of divergence of *Eubalaena* from the

61 bowhead whale (McLeod et al., 1993; Santangelo et al., 2005).

62 The fossil record of *Eubalaena* is scanty and scattered around the northern hemisphere. A right

63 whale skull from the Pleistocene of Japan was described by Nishiwaki & Hasegawa (1969) and

64 reviewed by Kimura (2009). Kimura (2009) also described *Eubalaena shinshuensis* from the latest

65 Miocene of the Gonda Formation, Nagano Prefecture, Japan. A partial skull of an indeterminate

66 species of *Eubalaena* was described by Bisconti (2002) from the Upper Pliocene of Tuscany,

67 Central Italy.

68 A large-sized balaenid skull from the "Merxemien" of Antwerp, northern Belgium, was described

69 by Plisnier-Ladame & Quinet (1969) who assigned it to *Balaena belgica*, a taxon established by

70 Abel (1941) based on a described and illustrated cervical complex and the mention of other cranial

71 remains. Bisconti (2003) questioned Abel's taxonomic decision and suggested that the skull should

72 be assigned to *Eubalaena*, a proposal supported by later phylogenetic analyses placing *'B.' belgica*

73 as sister-group to *E. glacialis* (Bisconti, 2005a; Churchill et al., 2012). However, a formal re-

74 description of the specimen is currently lacking and this makes it dubious every new taxonomic

75 assignment.

76 The specimens previously assigned to *'Balaena' belgica* consist (1) a cervical vertebrae

77 complex discovered on March 6th, 1914 by G. Hasse in the docks of the Antwerp harbor, figured

78 by Abel (1941, pl. 2) and Plisnier-Ladame & Quinet (1969, fig. 1), and bearings the inventory

79 number of the Royal Belgian Institute of Natural Sciences, Brussels (hereinafter RBINS) RBINS

80 M. 881 (IG 8444); (2) a partial neurocranium discovered in 1921 in Oorderen (a part of the

81 Antwerp harbor) during the excavation of the first Kruisschans lock (Figs. 1 and 2), figured by

82 Plisnier-Ladame & Quinet (1969, pl. 1-2), and bearing the inventory number RBINS M. 879a-f

83 (IG 8652); (3) a large fragment of right maxilla also discovered in 1921 in Oorderen during the

84 excavation of the first Kruisschans lock seemingly misidentified as a fragment of mandible by

85 Plisnier-Ladame & Quinet (1969), but never described or figured, and bearing the inventory

86 number RBINS M. 880a-c (IG 8652); and (4) a large isolated left humerus without any locality

87 data, most likely corresponding to the specimen mentioned by Plisnier-Ladame & Quinet (1969),

88 but never described or figured, and bearing the inventory number RBINS M. 2280.

89 In this paper, the material previously assigned to *'Balaena' belgica* Abel, 1941 is newly described

90 and compared with an extended sample of right, bowhead and pygmy right whales to get a

91 comprehensive analysis of anatomy and clear taxonomic assignments. The morphological

92 characters of the skull are then used in a new phylogenetic analysis of living and fossil right and

93 bowhead whales (1) to get information about the timing of the origin of the genus *Eubalaena* and

94 the divergence time from its closest living relative *Balaena mysticetus*, and (2) to investigate

95 whether the three living right whale populations correspond to three different species confirming

96 or not the results of molecular analyses. Our results will hopefully provide molecular ecologists

97 with useful information for safer reconstructions of past population dynamics of these highly

98 endangered species.

99

100 **Materials and methods**

101 *Institutional abbreviations*

102 AMNH, American Museum of Natural History, New York, USA. IZIKO, IZIKO Natural History

103 Museum, Cape Town, South Africa. MSNT, Museo di Storia Naturale e del Territorio, Università

104 di Pisa, Calci, Italia. NBC, Naturalis Biodiversity Center, Leiden, The Netherlands. RBINS, Royal

105   Belgian Institute of Natural Sciences, Brussels, Belgium. Additional abbreviations are provided in

106   the Supplementary Information file.

107

108   *New species name*

109   The electronic version of this article in Portable Document Format (PDF) will represent a

110   published work according to the International Commission on Zoological Nomenclature (ICZN),

111   and hence the new names contained in the electronic version are effectively published under that

112   Code from the electronic edition alone. This published work and the nomenclatural acts it contains

113   have been registered in ZooBank, the online registration system for the ICZN. The ZooBank

114   LSIDs (Life Science Identifiers) can be resolved and the associated information viewed through

115   any standard web browser by appending the LSID to the prefix http://zoobank.org/. The LSID for

116   this publication is: urn:lsid:zoobank.org:pub:C8D3FE95-303E-4EF4-86DD-1B453E124981. The

117   online version of this work is archived and available from the following digital repositories: PeerJ,

118   PubMed Central and CLOCKSS

119

120   *Anatomy*

121   Anatomical terms about skull osteology follow Mead and Fordyce (2009); terminology for

122   humerus and cervical vertebrae follows Schaller (1999).

123

124   *Comparative analyses*

125   Comparative analyses were made with an extended balaenoid sample including specimens from

126   museums MSNT, RBINS, AMNH, and IZIKO. In addition, specimens described in literature were

127   used to complement first-hand observations (True, 1904; Omura, 1958; Tomilin, 1967).

128

129 *Body size estimate*

130 Three methods for body size estimate were followed. First, we used the regression equation

131 provided by Pyenson & Sponberg (2011) that allows the reconstruction of the total body length

132 based on a measure of the bizygomatic width of the skull. The equation is the following:

133 $$(1) \log (TL) = 0.92(\log (BIZYG) - 1.64) + 2.67$$

134 In the equation (1), abbreviations are as follows: TL, total body length; BIZYG, bizygomatic

135 width. Pyenson & Sponberg (2011) used this equation to reconstruct total body lengths of living

136 and fossil cetaceans including mysticetes. Unfortunately, their study did not involve

137 reconstructions of balaenid body length, therefore we cannot be sure that the equation (1) is well

138 suited to provide an accurate reconstruction of the total body length for the extinct balaenid RBINS

139 M. 879a-f. Moreover, bizygomatic width was found to generate results that, as a whole, deviated

140 from observed values of intact specimens for amounts ranging from 47 to 37%. Bearing this in

141 mind, we corrected our results generated by the equation (1) by reducing what we found by 47 and

142 37%; in so doing, we got two results from applying the equation (1) that correspond to the range

143 of estimates for the total body length of RBINS M. 879a-f.

144 The second method applied to infer body mass and body length of RBINS M. 879a-f used the

145 occipital breadth as principal predictor as from the following equation, provided by Evans et al.

146 (2012):

147 $$(2) BM = 4.924 * 10^{-6}(OCB)^{3.858}$$

148 In the equation (2), the abbreviations are as follows: BM, body mass (in Kg); OCB, occipital

149 breadth (in mm). The equation (2) showed a high correlation coefficient in mammals ($R^2 =$

150 0.9447). Once a body mass estimate was obtained from the equation (2), we used equation (3) to

151   obtain an estimate of skeletal length. Equation (3) is the following, as developed by Silva &

152   Downing (1995):

153     $$(3)\ \log(BM) = 3.08(\log(SL)) - 4.84$$

154   Abbreviations used in equation (3) are the following: BM, body mass; SL, skeletal length. This

155   equation was extensively used in the reconstructions of body masses and skeletal lengths of living

156   and fossil mammals in previously published papers.

157   Unfortunately, none of these equations was tested on balaenid records and it is not known if they

158   are actually able to retrieve correct results in this family. For this reason, we used also the

159   regression equation provided by Bisconti (2002) to predict the total skull length of a balaenid whale

160   based on supraoccipital length. The equation is the following:

161     $$(4)\ SuL = 0.3937(SkL) - 62.803$$

162   The abbreviations used in the equation (4) are the following: SuL, supraoccipital length; SkL, total

163   skull length (i.e., condylobasal length). Unfortunately, the correlation coefficient associated to this

164   equation is rather low ($R^2 = 0.5967$) because the regression equation is based on a limited and

165   scattered dataset. Once a condylobasal length is obtained by using the equation (4), we inferred

166   the total body length by tripling or quadrupling the condylobasal length. In fact, following Tomilin

167   (1967), the skull length is about 25-to-30% of the total body length in extant Balaenidae. Presently

168   it is not possible to be sure that this proportion applies to a given fossil balaenids; however, given

169   that skull and body sizes have important adaptive functions in Balaenidae (Sanderson &

170   Wassersug, 1993), and given that RBINS 879a-f represents an advanced balaenid species (as

171   judged from its placement in the phylogenetic hypothesis of relationships presented in this paper),

172   there is no reason to propose a fundamentally different skull/body ratio in this specimen.

173

174   *Phylogenetic analysis*

175   A total of 153 morphological characters were coded for 42 taxa including 3 archaeocetes used as

176   outgroups. The taxonomic sampling adopted here includes representative taxa from all the known

177   mysticete radiations. The family Balaenidae was represented by 11 taxa including *Morenocetus*

178   *parvus*; Neobalaenidae was represented by *Caperea marginata* and *Miocaperea pulchra*.

179   *Eubalaena shinshuensis* and the Pliocene *Eubalaena* sp. from Tuscany were included in a

180   phylogenetic analysis for the first time.

181   Characters were coded based on direct examination of specimens and on the literature listed in the

182   Supplementary Information file together with both character list and taxon x character matrix.

183   Only 2 characters were coded from baleen morphology; all the other characters were coded from

184   the analysis of the skeletal anatomy of mysticetes and archaeocetes. All characters were unordered

185   and unweighted and followed the outgroup polarization criterion.

186   Character choice was made bearing in mind the goal of maximum reduction of homoplasy in the

187   dataset. This goal was achieved by examining the homoplasy level shown by each character states

188   published by Bisconti (2008, 2011), Bisconti et al. (2013), Bisconti & Bosselaers (2016), Marx

189   (2011) and Boessenecker & Fordyce (2015). Bisconti et al. (2013) and Bisconti & Bosselaers

190   (2016) published the consistency index (hereinafter abbreviated as CI) of all the synapomorphies

191   supporting named nodes. Characters with CI < 1 were considered homoplastic and were excluded

192   from the present dataset. As far as characters from other papers are concerned, it was more difficult

193   to decide whether a character had a homoplastic distribution or not. To get decisions, character

194   states were mapped on published phylogenetic hypotheses and their distributions were assessed by

195   eye; in the case a character showed scattered distribution across the branches of the Mysticeti tree,

196   then the application of Fitch's (1971) parsimony allowed to decide if the character could be

197   considered homologous or not in those branches.

198 The taxon **x** character matrix was treated by TNT (Goloboff et al., 2008) with default parameters

199 for New Technology Search. The synapomorphies were mapped onto the resulting cladogram and

200 were listed through the dedicate commands in TNT. Number of steps added by each character was

201 calculated at relevant nodes to determine whether the character state constituted an ambiguous or

202 unambiguous synapomorphy at the node.

203

204 *Stratigraphic consistency index and determination of divergence dates*

205 The degree of agreement between the branching pattern and the stratigraphic occurrence of the

206 taxa was assessed by the calculation of the Stratigraphic Consistency Index (hereinafter, SCI)

207 following the method described by Huelsenbeck (1994; see also discussion in Bisconti, 2007).

208 Stratigraphic ages of the taxa were obtained from the Paleobiology Database available at

209 https://paleobiodb.org and mainly compiled by Mark Uhen. Adjustments to the ages of the

210 specimens provided by Marx & Fordyce (2015) were also included were necessary. Stratigraphic

211 ages of the taxa are provided in the Supplementary Information file published in the website of

212 this Journal. The stratigraphic intervals of occurrence of the taxa were used to constrain the

213 divergence dates of the branches included within Balaenoidea in order to get information about

214 the origin of the living right whale and bowhead whale species.

215

216 **Systematic Paleontology**

217

218 Class MAMMALIA Linnaeus, 1758

219 Order CETACEA Brisson, 1762

220 Suborder MYSTICETI Cope, 1891

221 Infraorder CHAEOMYSTICETI Mitchell, 1989

222 Parvorder BALAENOMORPHA Geisler & Sanders, 2003

223 Superfamily BALAENOIDEA Flower, 1865

224 Family BALAENIDAE Gray, 1825

225

226 Balaenidae gen. et sp. indet.

227

228 *Material*. Cervical vertebrae complex RBINS M. 881 (IG 8444).

229

230 *Locality and horizon information*. The specimen was found on March 6, 1914 by G. Hasse in the

231 docks of Antwerp harbor (northern Belgium), more precisely in the "darses I-II" (Fig. 1). Abel

232 (1941) mentions an origin in the "Scaldisien" for this specimen. Now disused, this

233 chronostratigraphic regional unit is roughtly equivalent to the Lillo Formation, a latest early to

234 Late Pliocene lithostratigraphic unit (Laga et al., 2006; see Fig. 2).

235

236 *Description*. The specimen includes a complex formed by fused cervical vertebrae (Fig. 3).

237 Anteriorly, only the ventral portions of the articular facets of the atlas for the occipital condyles of

238 the skull are preserved. The articular surfaces of the facets are highly concave and wide

239 (measurements are provided in Table 1). The articular facets are separated dorsally by a wide

240 concavity that corresponds to the ventral border of the neural canal. Posteriorly, the articular facet

241 of the 7th cervical vertebra for the 1st thoracic vertebra is highly concave and shows a uniformly

242 convex lateral border. Laterally, the ventral apophysis of the atlas protrudes laterally and ventrally

243 and is separated from a small fragment of the ventral apophysis of the axis by a narrow,

244   dorsoventral groove that is slightly oblique in lateral view. The transverse grooves that are

245   sometimes observed in the cervical complexes of *Caperea marginata* and in balaenid species

246   (Bisconti, 2012) are not seen in this specimen. No additional characters can be described due to

247   the poor preservation of the specimen.

248

249   *Discussion and taxonomic decision.* The specimen represents a complex that presumably includes

250   all the cervical vertebrae of a balaenid whale. The morphology is consistent with that of Balaenidae

251   as in *Caperea marginata* the ventral apophysis projects much more ventrally and the outline of the

252   posterior articular surface of the 7th cervical vertebra is squared in posterior view. In other

253   mysticetes the cervical vertebrae are not fused; fusion may occasionally occur in the presence of

254   pathological processes, but the involvement of all the cervical vertebrae is extremely rare. It is

255   possible to distinguish the cervical vertebrae of the living species of *Eubalaena* from the extant

256   *Balaena mysticetus* based on: (1) shape of the neural apophysis, (2) shape of the neural canal, and

257   (3) size, shape and orientation of the ventral apophysis of the atlas. Unfortunately, the specimen

258   RBINS M. 881 is too poorly preserved to allow a safe identification; in fact, in this specimen the

259   neural apophyses are not preserved, the neural canal is only partly preserved, and the ventral

260   apophyses of the atlas are largely damaged and worn. For this reason, we assign RBINS M.881 to

261   Balaenidae gen. et sp. indet. Consequently, this decision implies that this specimen cannot be

262   designated as the holotype of the species *Eubalaena belgica*. Therefore, as Abel (1941) designated

263   RBINS M. 881 as the type of '*Balaena belgica* and now we assign it to gen. et sp. indet., it follows

264   that both '*Balaena belgica* and its recombination, *Eubalaena belgica*, are nomina dubia.

265

266   Balaenidae gen. et sp. indet.

267

268 *Material.* Fragment of right maxilla RBINS M. 880a-c (IG 8652)

269

270 *Locality and horizon information.* The specimen was found at Oorderen during the excavation of

271 the first Kruisschans lock of the Antwerp harbor at a depth of 7.80 m under the sea level (Fig. 1).

272 The specimen originates from the Lillo Formation ("Scaldisien"), in a level slightly lower than the

273 neurocranium RBINS M. 879 (see below). Its geological age falls in the range 3.7-2.8 Ma (latest

274 Zanclean-Piacenzian; De Schepper et al., 2009; Fig. 2).

275

276 *Description.* The specimen includes part of the proximal portion of the right maxilla of a balaenid

277 whale (measurements are provided in Table 1). The maxilla is transversely compressed and bears

278 an arched and thin lateral border (Fig. 4). Posteriorly, three infraorbital foramina are observed;

279 ventrally a long groove for the vasculature of the baleen-bearing tissue runs along the whole ventral

280 surface of the bone. Such a surface is lateromedially and anteroposteriorly concave. It is not clear

281 if the orientation of this fragment is more similar to *Eubalaena* and *Balaenula* (in these taxa the

282 posterior portion of the maxilla is nearly horizontal in lateral view) or to *Balaena mysticetus* (in

283 this species the posterior portion of the maxilla projects dorsally and anteriorly) or to *Balaenella*

284 *brachyrhynus* (in this species the posterior portion of the maxilla distinctly projects

285 anteroventrally).

286

287 *Discussion and taxonomic decision.* The specimen RBINS M. 880a-c represents a balaenid

288 maxilla. In fact it shows a distinctive arch in lateral view, it is transversely compressed, and it

289 displays a longitudinally-developed groove for the vasculature of the baleen-bearing tissue.

290 Unfortunately, it is impossible to reconstruct the original orientation of this fragment in the skull;

291 this, together with the lack of the anterior portion of the rostrum and of the lateral process of the

292 maxilla, prevents a safe taxonomic assignment. For this reason, we assign RBINS M. 880a-c to

293 Balaenidae gen. et sp. indet.

294

295 Genus *Eubalaena* Gray, 1864

296

297 *Type species. Eubalaena australis* Desmoulins, 1822.

298

299 *Emended diagnosis of genus*. Balaenid cetacean characterized by all the characters diagnostic of

300 the *Eubalaena + Balaenula* clade (i.e., rostrum and supraorbital process of the frontal form a right

301 angle in lateral view, nasal and proximal rostrum horizontal in lateral view, orbitotemporal crest

302 well developed on the dorsal surface of the supraorbital process of the frontal, and zygomatic

303 process of the squamosal directed anteriorly so that the posterior wall of the temporal fossa cannot

304 be observed in lateral view) and by the following, exclusively *Eubalaena* characters: vertically-

305 oriented squamosal, protruding lambdoid and temporal crests, convex and protruding

306 supramastoid crest, dome-bearing supraoccipital, wide and rounded anterior process of

307 supraoccipital, and pars cochlearis of petrosal protruded cranially.

308

309 *Discussion.* Bisconti (2003) provided the last diagnosis of *Eubalaena* published up to the present

310 work; diagnostic characters included: gigantic body size (maximum body length approaching 22

311 m), rostrum and supraorbital process of frontal form a right angle, nasal and proximal rostrum

312 horizontal, ascending temporal crest well developed on the dorsal surface of the supraorbital

313   process of the frontal, vertically-developed squamosal, zygomatic process of the squamosal

314   directed anteriorly so that the posterior wall of the temporal fossa cannot be observed in lateral

315   view, protruding lambdoidal and temporal crests, convex and protruding lateral squamosal crest,

316   exoccipital squared in lateral view, dome-bearing supraoccipital shield with sagittal crests, wide

317   anterior process of supraoccipital, pars cochlearis cranially-protruding, and superior process of

318   petrosal cranially-protruding. Bisconti's (2003) diagnosis is certainly useful to separate extant

319   *Eubalaena* from other living balaenids but it may be of limited help when trying to separate fossil

320   *Eubalaena* species from other living and fossil balaenids. In particular, the above diagnosis

321   includes characters that are shared with the extinct *Balaenula* lineage: rostrum and supraorbital

322   process form a right angle, nasal and proximal rostrum horizontal, ascending temporal crest

323   (orbitotemporal crest *sensu* Mead & Fordyce, 2009) well developed on the dorsal surface of the

324   supraorbital process of the frontal, and exoccipital squared in lateral view. All these characters can

325   be observed also in *Balaenula astensis* or in *Balaenula balaenopsis*. A more detailed diagnosis of

326   *Eubalaena* allowing to separate this genus from all the other living and extinct balaenid taxa

327   includes the characters listed in the Emended diagnosis of genus provided above.

328

329   *Eubalaena* sp. indet.

330

331   *Material.* Left humerus RBINS M. 2280.

332

333   *Locality and horizon information*. Antwerp area. There is no precise locality data available for this

334   specimen. A stratigraphic assessment is currently impossible.

335

336   *Description.* This well-preserved, robust left humerus shows a highly rounded proximal articular

337   head that is anteriorly bounded by a protruding deltoid tuberosity; the latter is triangular in lateral

338   view (measurements are provided in Table 1). The diaphysis shows straight anterior and posterior

339   borders (Fig. 5); the posterior border is shorter than the anterior border, as it terminates more

340   proximally due to the development of the articular facet for the olecranon process of the ulna. Such

341   a facet protrudes posteriorly and occupies part of the posterior border of the humerus. The

342   anteroventral corner of the humerus protrudes anteriorly forming a kind of triangular tuberculum.

343   The articular facets for radius and ulna are separated by a transverse protrusion that is triangular

344   in lateral view.

345

346   *Discussion and taxonomic decision.* The morphology of the articular head of the humerus RBINS

347   M. 2280 is consistent with both *Eubalaena* and *Balaena*. In *Eubalaena glacialis* the external

348   border of the lateral surface of the articular head shows a posterior concavity that is not seen in

349   *Balaena mysticetus* (Benke, 1993). Unfortunately, RBINS M. 2280 is worn in that region thus

350   preventing a clear understanding of its morphology. More distally, the articular facet for the

351   olecranon is well developed as seen in the extant *Eubalaena* species while in *Balaena mysticetus*

352   it is largely reduced. Benke (1993) showed that the posterior border of the diaphysis in *Balaena*

353   *mysticetus* is uniformly concave and short and that the deltoid tuberosity is less protruding than in

354   *Eubalaena glacialis*. In the latter, the posterior border of the diaphysis is more elongated

355   (resembling that of RBINS M. 2280) and the deltoid tuberosity is triangular and protruding. In the

356   humerus RBINS M.2280 the deltoid tuberosity is triangular and protruding as in *E. glacialis*.

357   However, the posterior border of the diaphysis of RBINS M. 2280 is straighter than that observed

358   in *E. glacialis*.

359   Comparative analysis shows, thus, that the humerus RBINS M. 2280 is closer to *Eubalaena* than

360   to *Balaena*, as it shares with *E. glacialis* the presence of (1) well-developed and protruding

361   articular facet for the olecranon process, (2) triangular and protruding deltoid tuberosity and, (3)

362   comparatively long posterior border of the diaphysis. These shared characters allow inclusion of

363   RBINS M. 2280 within *Eubalaena*. However, the different shape of the posterior border of the

364   diaphysis and the lack of information about the shape of the lateral outline of the articular head do

365   not allow inclusion of this specimen within *E. glacialis* or other extant *Eubalaena* species. RBINS

366   M. 2280 is thus assigned to *Eubalaena* sp. indet.

367   When compared to the extant *Eubalaena* species, this humerus is particularly long suggesting that

368   it belonged to a big individual. The total proximodistal length of RBINS M. 2280 is 683 mm,

369   which is greater than the maximum humeral lengths published by Benke (1993) for *Balaena*

370   *mysticetus*, *Eubalaena glacialis*, and *E. australis*, and by Omura (1958) for *E. japonica*. Based on

371   this comparison, we suggest that the humerus RBINS M. 2280 belonged to an individual that was

372   longer than 16.5 m. This is the first report of a gigantic right whale in the fossil record of the North

373   Sea.

374

375   *Eubalaena ianitrix* sp. nov. LSID: urn:lsid:zoobank.org:act:F17C4DCA-FF1B-4EA4-9E6B-

376   6C1EED448745

377

378   *Derivation of name.* The specific name *ianitrix* derives from Ianus, the Roman God who was the

379   guardian of passages, gates and doors. This name is related to the discovery of the holotype in the

380   locks (or entrances) of the Antwerp harbor.

381

382 *Holotype.* The holotype is housed at the Royal Belgian Institute of Natural Sciences, Brussels,

383 Belgium, and bears the inventory number M. 879a-f, Reg. 4019, I.G. 8652 (all the numbers refer

384 to the same individual). It includes a partial skull (M. 879a), right squamosal and exoccipital (M.

385 879b), left squamosal and exoccipital (M. 879c), fragment of a maxilla (M. 879d), fragment of the

386 right supraorbital process of the frontal (M. 879e), fragment of the left supraorbital process of the

387 frontal (M. 879f).

388

389 *Type locality.* The neurocranium RBINS M. 879a-f was discovered in Oorderen (Fig. 1) during

390 the excavation of the first Kruisschans lock (*'première écluse du Kruisschans'*, now named Van

391 Cauwelaertsluis) of the Antwerp harbor (Plisnier-Ladame & Quinet, 1969). Geographic

392 coordinates: 51°16'32"N- 04°19'51"E. As mentioned above, the maxilla RBINS M. 880a-c was

393 found at the same site. However, based on labels associated to specimens, the neurocranium was

394 found at a depth of 3.70 m under the sea level, whereas the maxilla was found at a depth of 7.80

395 m under the sea level, therefore most likely not representing the same individual.

396

397 *Type horizon.* Based on data associated to the neurocranium RBINS M. 879a-f, Misonne (1958)

398 indicated an origin in the Kruisschans Sands (*'Sables du Kruisschans'*; Fig. 2) in the *'zone à*

399 *Cardium'*, and a Merksemian ('Merxemien') stage, a stage assignation later confirmed by Plisnier-

400 Ladame & Quinet (1969). Now disused, this regional stage was first introduced by Heinzelin

401 (1955a), including the Kruisschans Sands and Merksem Sands, together with an underlying gravel

402 layer (Laga & Louwye, 2006). Both the Kruisschans Sands Member and Merksem Sands Member

403 are now part of the Lillo Formation, constituting its two youngest members (Vandenberghe et al.,

404 1998; Laga et al., 2006).

405 In published sections of the Pliocene and Quaternary layers at the Kruisschans locks (including

406 sections in a new lock parallel to the ancient lock, 'Ecluse Baudouin'), a clayey sand layer

407 containing a high concentration of shells of the bivalve *Laevicardium* (first named *Cardium*)

408 *parkinsoni* and isolated cetacean bone fragments is reported at a depth of 5.5-7 m (Heinzelin, 1952,

409 1955b). This shell layer is located about 1 m above the base of the Kruisschans Sands. It is

410 therefore tempting to propose that the 'zone à *Cardium*' mentioned by Misonne (1958) for the

411 horizon of the skull RBINS M. 879a-f corresponds to this part of the Kruisschans Sands.

412 Dinoflagellate cysts from a section 4 km north to the Kruisschans locks give a Piacenzian (Late

413 Pliocene) age to both the Kruisschans Sands Member and the overlying Merksem Sands Member,

414 older than 2.6 Ma (as confirmed by pollens) and most likely somewhat younger than 3.7 Ma (age

415 of the base of the Lillo Formation), whereas sequence stratigraphy narrows even more their

416 temporal range to 3.2 to 2.8 Ma (De Schepper et al., 2009). RBINS M. 879a-f is therefore proposed

417 to date from that Piacenzian interval.

418 The record of fossil marine mammals in the Kruisschans Sands Member is relatively poor; only

419 the odobenid *Alachtherium antwerpiensis* and the stem phocoenid *Septemtriocetus bosselaersi* are

420 known to originate from that unit (Hasse, 1909; Lambert, 2008).

421

422 *Diagnosis. Eubalaena ianitrix* differs from *E. shinshuensis* in showing a distinctive anteroventral

423 corner in the parietal-frontal suture and in having an anterodorsally protruded squamosal-parietal

424 suture; it differs from the *Eubalaena* sp. from the early Late Pliocene of Tuscany in having an

425 anteriodorsally protruded squamosal-parietal suture; it differs from *E. japonica* in having the

426 pterygoid exposed in the temporal fossa, in having posteromedially directed anterior borders of

427 the palatine and in having anteriorly directed posterior borders of the palatine; it differs from *E.*

428   *australis* in having a differently shaped anteroventral corner in the parietal-frontal suture, in having

429   an anterodorsally protruded squamosal-parietal suture, in having the pterygoid exposed in the

430   temporal fossa and in having anteriorly directed posterior border of the palatine; it differs from *E.*

431   *glacialis* in having a crest located at the squamosal-parietal-supraoccipital suture and in having

432   anteriorly directed posterior border of the palatine.

433

434

435

436   **Comparative anatomy**

437

438   The holotype specimen consists of a moderately well preserved partial skull. The skull is massive

439   and heavy and lacks part of the supraoccipital borders due to post-mortem erosion. It is subdivided

440   into six fragments that can be put together due to clear break surfaces. Measurements are provided

441   in Table 2.

442

443   *Rostrum.* Only a fragment of the right maxilla is preserved showing the typical transverse

444   compression of Balaenidae.

445

446   *Frontal.* Due to the erosion of the anterior-most border of the supraoccipital, it is possible to

447   observe a tiny portion of the interorbital region of the frontal in dorsal view (Figs 6). Prior to the

448   erosion of the supraoccipital, that portion was superimposed by the anterior portion of the

449   supraoccipital and was not visible. Judging from what is preserved, the interorbital region of the

450   frontal was less bent than the supraoccipital suggesting that, in lateral view, the posterior portion

451   of the rostrum was nearly flat as seen in *Eubalaena glacialis*. The transverse diameter of the

452   interorbital region (measured along the inferred position of the nasofrontal suture) is *c.* 240 mm.

453   The supraorbital processes of the frontal are detached from the skull probably because post-

454   mortem damage. The supraorbital process of the frontal is anteroposteriorly narrow and bears an

455   evident but rounded orbitotemporal crest developed from the postorbital process to its

456   anteromedial border (Figs 6, 7 and 8). The orbitotemporal crest is sharper proximally and becomes

457   lower approaching the orbital rim. The right supraorbital process of the frontal is 650 mm in length

458   up to the center of the orbit. The left supraorbital process of the frontal is 712 mm in length. A

459   long groove for articulation with the maxilla is located at the anteromedial corner of the left

460   supraorbital process of the frontal (Fig. 9).

461   The optic canal is deep proximally (depth is *c.* 45 mm) and shallow distally (depth is *c.* 35 mm).

462   Proximally, the right optic canal is bordered by anterior and posterior crests whose distance is 50

463   mm proximally and *c.* 100 mm distally (Fig. 10). The anteroposterior diameter of the left optic

464   canal is 30 mm proximally at a distance of 400 mm from the orbital rim and 70 mm a few mm

465   from the orbital rim.

466   Approaching the orbit, the dorsal surface of the supraorbital process of the frontal flattens. The

467   right orbit is 170 mm in length (from the center of the postorbital process of the frontal to the

468   center of the antorbital process of the frontal) and 51 mm in height (measured from the center of

469   the orbital rim to an imaginary line joining antorbital and postorbital processes of the frontal). On

470   the right side, antorbital and postorbital processes are similar in size but on the left side, the

471   postorbital process is more robust than the antorbital process (Figs 7 and 8). The longitudinal axis

472   of the supraorbital process of the frontal is perpendicular to the imaginary line joining antorbital

473   and postorbital processes. This suggests that, in the living animal, the supraorbital process of the

474 frontal formed an approximately right angle with the lateral process of the maxilla and, thus,

475 resembling the condition observed in the right whale of the genus *Eubalaena* and the fossil

476 *Balaenula*.

477 The frontal of *Eubalaena ianitrix* shares the following characters with the living *Eubalaena* and

478 *Balaenula*: presence of an evident orbitotemporal crest developed from the postorbital process to

479 the anteromedial corner of the supraorbital process of the frontal, lack of dorsoventral compression

480 along most of the length of the supraorbital process of the frontal (as seen in *Morenocetus parvus*,

481 *Balaena mysticetus* and *Balaenella brachyrhynus*), presence of a right angle between supraorbital

482 process of the frontal and the lateral process of the maxilla in lateral view, interorbital region of

483 the frontal clearly angled with respect to the dorsoventral inclination of the supraoccipital. The

484 articular groove for the maxilla combined with the short anteroposterior diameter of the proximal

485 portion of the supraorbital process suggests that the ascending process of the maxilla was short

486 and wide like that typically observed in the other Balaenoidea where this structure has been

487 described (Bisconti, 2012 and literature therein). The short exposure of the interorbital region of

488 the frontal on the dorsal surface of the skull and the exclusion of the parietal from exposure at

489 cranial vertex are typical characters of living and fossil Balaenoidea.

490

491 *Parietal.* The parietal is evident on the lateral sides of the skull and at the cranial vertex due to the

492 erosion of the anterior-most border of the supraoccipital (Fig. 6). Originally, the parietal was

493 covered by the anterior border of the supraoccipital forming the nuchal crest. The frontal border

494 of the parietal is superimposed on the interorbital region of the frontal obliterating it in dorsal view.

495 More laterally, the frontal border descends ventrally and posteriorly and borders the posterodorsal

496 portion of the supraorbital process of the frontal and forming an anteriorly convex coronal suture.

497   Posteriorly to the supraorbital process of the frontal, the coronal suture forms a curve with anterior

498   concavity and projects ventrally and posteriorly (Figs 7, 8).

499   The shape of the coronal suture is different in different balaenoid lineages. In the skull of *Caperea*

500   *marginata* as seen in lateral view, the frontal border of the parietal gently descends from an

501   anterodorsal point to a point located posterventrally in a straight-to-slightly convex line located

502   dorsally to the supraorbital process of the frontal. This shape of the frontal border of the parietal

503   is shared also with *Balaena mysticetes*, *B. montalionis*, *B. ricei* and *Balaenella brachyrhynus*. In

504   the fossil *Miocaperea pulchra*, the right parietal shows a slightly different condition; in this species

505   a distinctive anteroventral corner is located along the frontal border of the parietal (Bisconti, 2012).

506   The anteroventral corner is present also in the species belonging to *Balaenula* and *Eubalaena* and

507   in *Eubalaena ianitrix* (Figs 7, 8). In *Eubalaena australis*, posterior to the anteroventral corner, the

508   frontal border shows a strong ventral concavity and a rounded shape making it distinct from the

509   parietal of all the other balaenoid species.

510   The supraoccipital border of the parietal protrudes laterally and, together with the lateral border of

511   the supraoccipital, forms the temporal crest. The temporal crest protrudes laterally and forms a sort

512   of short roof of the temporal fossa in such a way that it prevents the medial wall of the temporal

513   fossa (formed by the external surface of the parietal) from being observed in dorsal view. The

514   external surface of the parietal is widely concave. Along the anteroposterior axis of the skull, the

515   parietal appears short and high. The dorsal portion of the squamous border is anteroposteriorly

516   elongated and bears a weak crest; the ventral portion of the squamous border forms a highly

517   interdigitated suture with the squamosal and projects ventrally.

518   Among Balaenidae, a crest along the squamous border has been detected as a synapomorphy of

519   *Balaena* and *Balaenella* by Bisconti (2005a) and Churchill et al. (2012) as it is absent from

520 *Balaenula* and *Eubalaena*. It is not clear whether this crest is present in *Morenocetus* and

521 *Peripolocetus*. The shape of the frontal border of the parietal differs from that observed in *Balaena*

522 and *Balaenella* as it shows an undulating development; in *Balaena* and *Balaenella* the frontal

523 border of the parietal proceeds posteroventrally as a straight line. A highly interdigitated ventral

524 portion of the squamous border of the parietal is also observed in a subadult individual of *E.*

525 *australis* (specimen NBC RGM 24757).

526 The squamous border of the parietal has distinctive characters in different balaenoid lineages. In

527 *Caperea marginata*, the dorsal portion of the squamous border projects posteriorly to meet the

528 supraoccipital (Bisconti, 2012). This character is also observed in *Balaena mysticetus* adult NBC

529 RGM 373 and foetal NBC RGM 31116; the character was also illustrated by Cuvier, 1823; see

530 Bisconti, 2003 for an image), *Eubalaena australis* adult IZIKO 2284, subadult NBC RGM 24757

531 and foetal IZIKO ZM 38950) and in the Pliocene *Eubalaena* sp. from Tuscany (Bisconti, 2002).

532 In *Miocaperea pulchra* and *Balaenella brachyrhynus* the dorsal portion of the squamous border is

533 nearly vertical. In *Eubalaena glacialis*, *E. japonica*, *Balaenula astensis* and *Eubalaena ianitrix* the

534 dorsal portion of the squamous border projects anteriorly forming a finger-like structure that is

535 deeply wedged between the parietal and the supraoccipital.

536

537 *Supraoccipital.* The supraoccipital is strongly built and represents the largest bone of this skull

538 (Fig. 6). Parts of the anterior and lateral borders are missing due to post-mortem erosion of the

539 skull. The supraoccipital is wide and, as preserved, shows convex lateral borders and widely

540 rounded anterior border. The anteroposterior length (from the anterior border to the inferred

541 position of the dorsal edge of the foramen magnum) is *c.* 531 mm; the transverse diameter is *c.*

542 350 mm anteriorly and *c.* 590 mm at mid-length. The external occipital protuberance, located on

543   the anterior surface of the supraoccipital, is dorsally convex and forms a wide dome bordered by

544   bilateral fossae located near the lateral borders of the supraoccipital. The dome consists of bilateral

545   relieves posteriorly separated by the interposition of a triangular, paraxial fossa. There is a low

546   sagittal crest located posteriorly to the dome. In lateral view, the dome is clearly visible as it

547   protrudes dorsally and is not obliterated to view by the temporal crests. Before the post-mortem

548   erosion of the skull, the supraoccipital formed a dorsal roof to the temporal fossa preventing the

549   parietal from being observed in dorsal view.

550   In the genus *Eubalaena*, the supraoccipital is anteriorly wide and rounded and displays an external

551   occipital protuberance that is dome-shaped. These characteristics of the supraoccipital are

552   observed in all the living *Eubalaena* species, in the fossil *E. shinshuensis* and in the *Eubalaena* sp.

553   described by Bisconti (2002) from the Pliocene of Tuscany. Subtle differences in the characters of

554   the dome could be used for differentiating the species of *Eubalaena* but it is not completely clear

555   whether the differences are due to individual variation or have taxonomic value. Bisconti (2002)

556   described a sagittal crest on the external occipital protuberance and a series of five parassial crests

557   posterior to it in a Pliocene *Eubalaena* sp. The five parassial crests are not observed in other

558   *Eubalaena* species. A single sagittal crest is present in *Eubalaena australis* (NBC RGM 24757),

559   *Eubalaena glacialis* (AMNH 42752, MSNT 264) *E. japonica* (Omura, 1958) and *Eubalaena*

560   *ianitrix*.

561   The external supraoccipital protuberance is formed by a bilateral bulge in *Eubalaena australis*

562   (NBC 24757), *E. glacialis* (AMNH 42752), *Eubalaena* sp. (Bisconti, 2002), and *E. ianitrix*, and

563   by a single axial bulge in *E. japonica* and *E. shinshuensis* (Kimura, 2009). The external

564   supraoccipital protuberance is a single bulge also in *Balaena mysticetus*, *Balaena montalionis*,

565   *Balaena ricei* and *Balaenella brachyrhynus* but in these species the anterior portion of the

566   supraoccipital is transversely constricted while in the species belonging to *Morenocetus*,

567   *Balaenula* and *Eubalaena* the anterior portion of the supraoccipital is transversely wide.

568   Observations on skulls belonging to living species suggest that the lateral borders of the

569   supraoccipital potentially undergo morphological change during ontogeny. In *Eubalaena*

570   *australis*, the lateral border of the supraoccipital is externally convex in foetal and subadult

571   individuals (ISAM ZM 38950, NBC RGM 24757). Omura (1958) observed that in adult

572   individuals of *Eubalaena glacialis* the lateral border of the supraoccipital is more concave that in

573   *E. japonica*. However, in the images provided by True (1904), an adult individual of *Eubalaena*

574   *glacialis* has a continuously convex lateral border of the supraoccipital. It is possible that the

575   Omura's (1958) observation was related to differences in the point of views from which the skulls

576   were observed.

577

578   *Vertex*. Based on Mead & Fordyce (2009, and literature therein) terminology, the vertex is the

579   highest portion of the skull. In mysticetes it is formed by a mosaic of bones including

580   supraoccipital, parietal, frontal and some posteromedial elements of the rostrum nasal and the

581   ascending process of the premaxilla and of the maxilla). In *E. ianitrix*, the supraoccipital is

582   superimposed onto the parietal and prevents it from being observed in dorsal view (Fig. 6). The

583   parietal is superimposed onto the interorbital region of the frontal that is, thus, scarcely visible in

584   dorsal view. The only portion of the interorbital region of the frontal that can be observed is that

585   that is immediately posterior to the nasofrontal suture. Judging from the articular groove present

586   on the anteromedial surface of the supraorbital process of the frontal, the ascending process of the

587   maxilla had a limited posterior extension resembling other living and fossil Balaenoidea.

588   The supraoccipital superimposition on the parietal and the parietal superimposition on the

589   interorbital region of the frontal are synapomorphies of Balaenidae and Neobalaenidae and are not

590   shared with other mysticete taxa (Bisconti, 2012 and literature therein). The lack of parietal

591   exposure at the cranial vertex is another exclusive feature of Balaenidae and Neobalaenidae and is

592   observed in all the living and fossil taxa belonging to these groups (Churchill et al., 2012; Bisconti,

593   2003).

594

595   *Exoccipital.* The lateral portion of the exoccipital is a wide and flat surface with external border

596   squared (Fig. 11). Only the left paroccipital process is preserved and appears strong and rugose in

597   ventral view. A squared external border of the exoccipital is observed in *Eubalaena japonica* and,

598   at a lesser extent, in *Eubalaena australis*. In *E. glacialis* the external border has a rounder shape

599   than in those species. In *Balaena mysticetus* and *B. montalionis* the external border of the

600   exoccipital appears anterolaterally round with a distinctive lateroventral corner that is observed

601   also in *E. glacialis* but that seems absent in *E. japonica* (Omura, 1958). In lateral view, the

602   exoccipital has a squared shape in *E. glacialis*, *E. australis*, *E. japonica* and the species belonging

603   to *Balaenula* but it is not clear whether a squared shape is also present in *Eubalaena ianitrix*.

604   The occipital condyle is wide, kidney-shaped and its surface for articulation with the atlas is nearly

605   flat along both the dorsoventral and the lateromedial axes. The main axis of the occipital condyle

606   is inclined from a posteroventral point to an anterolateral point. There is a wide ventral concavity

607   separating the condyles. The condyles are not in contact each other ventrally or dorsally. The

608   maximum anteroposterior diameter of the occipital condyle is 190 on the right side and 170 on the

609   left side; the maximum lateromedial diameter of the occipital condyle is 101 on the right side and

610   107 on the right side. The condyles surround a wide foramen magnum whose dorsal border is not

611 preserved. The maximum tansverse diameter of the foramen magnum is 145 mm and its

612 anteroposterior diameter is inferred to be *c.* 140 mm based on a nearly circular outline with a slight

613 dorsoventral compression as seen in other balaenid species. The distance between the external

614 borders of the occipital condyles is *c.* 350 mm.

615

616 *Squamosal.* Right and left squamosals are partly broken; breakage lines are straight enough to

617 allow an easy reconstruction of this part of the skull by putting the broken portions of the

618 squamosals in place through right connections (Figs 7, 8).

619 The parietal margin of the squamosal forms the squamosal-parietal suture. Dorsally, this suture

620 projects anteriorly making it possible for the squamosal to be deeply inserted between the

621 supraoccipital and the parietal. More ventrally, the squamosal-parietal suture is highly

622 interdigitated.

623 The squamosal plate is dorsoventrally and anteroposteriorly concave and, in lateral view, it is

624 hidden by the anterior and ventral development of an anteriorly convex supramastoid crest. The

625 supramastoid crest is protruding anterolaterally and shows a widely rounded anterior shape. The

626 supramastoid crest is separated from the zygomatic process of the squamosal by a wide anterior

627 concavity. The zygomatic process of the squamosal is short and stocky. It projects laterally and

628 ventrally.

629 The squamosal has a clear dorsoventral development as it is typically observed in Balaenidae. Its

630 dorsoventral diameter is 550 mm on the external surface (from the exoccipital-squamosal suture

631 to the anterior end of the zygomatic process of the squamosal) of the right squamosal. The glenoid

632 fossa of the squamosal is largely eroded; what remains suggests that it was flat or scarcely concave

633   as seen in other typical balaenid whales. The glenoid fossa of the right squamosal is 470 mm in

634   anteroposterior length.

635   Posterodorsally, the tympanosquamosal recess is developed ventrally to the exoccipital-squamosal

636   suture and is ventrally bordered by a crest that separates it from the external acoustic meatus. Both

637   the tympanosquamosal recess and the external acoustic meatus are represented by transverse and

638   tube-like concavities developed along the dorsal and posterior portion of the squamosal.

639   The falciform process is developed ventrally and anteriorly. It forms the posterior border of the

640   foramen ovale which is included between squamosal and pterygoid.

641   The squamosal of *Eubalaena ianitrix* shows the following typical balaenid characters: dorsoventral

642   elongation, reduction of the zygomatic process of the squamosal, scarcely concave glenoid fossa

643   of the squamosal, widely rounded supramastoid crest. The short zygomatic process of the frontal

644   is also shared with *Caperea marginata*. In *Balaenella* and in the species of *Balaena* the squamosal

645   is also posteroventrally oriented (Bisconti, 2000) but this character is not observed in *E. ianitrix*.

646   Rather, the squamosal of *E. ianitrix* appears more vertical resembling *Morenocetus*, *Balaenula* and

647   the living species of *Eubalaena*. In *Balaenella brachyrhynus*, *Balaena mysticetus*, *B. ricei*, and *B.*

648   *montalionis*   the zygomatic process of the squamosal projects more laterally allowing the view of

649   the posterior wall of the temporal fossa formed by the squamosal plate. In *Eubalaena*, *Balaenula*

650   and *E. ianitrix* this is not the case as the zygomatic process of the squamosal projects anteriorly

651   and prevents the posterior wall of the temporal fossa from being observed in lateral view.

652

653   *Alisphenoid.* The alisphenoid is exposed in the temporal fossa. It has a triangular shape. It is

654   bordered anteriorly by the posterior border of the supraorbital process of the maxilla, ventrally by

655   the palatine, dorsally and posteriorly by the squamosal.

656 The alisphenoid is exposed in the temporal fossa in *Eubalaena glacialis* and *E. japonica* but it is

657 not clear whether such an exposure occurs also in *E. australis*. In foetal specimen (IZIKO ZM

658 38950) the alisphenoid is observed in the temporal fossa but in subadult individual (NBC RGM

659 24757) the alisphenoid is only visible in ventral view and does not appear in the temporal fossa as

660 the ventral border of the squamosal superimposes onto it. In *Balaena mysticetus*, *B. brachyrhynus*,

661 and in the genus *Balaenula* the alisphenoid is inferred to be exposed in the temporal fossa based

662 on the articular pattern of squamosal and parietal. The alisphenoid was originally bordered by the

663 squamosal dorsally and posteriorly and by the parietal dorsally and anteriorly, by the palatine

664 ventrally.

665

666 *Temporal fossa.* The temporal fossa of *E. ianitrix* is dorsally overhung by the lateral projection of

667 the temporal crest formed by the lateral border of the supraoccipital and the dorsal border of the

668 parietal (Fig. 6). The lateral extension of the temporal crest is not clear because the lateral edge of

669 the supraoccipital and the dorsal border of the parietal are worn. The medial wall of the temporal

670 fossa is formed by parietal, squamosal and alisphenoid. The alisphenoid is not in contact with the

671 parietal; the parietal-squamosal suture is highly interdigitated ventrally but, dorsally, the

672 squamosal forms a digit-like anterior protrusion that is deeply inserted between the supraoccipital

673 and the parietal. The medial wall of the temporal fossa is concave both dorsoventrally and

674 anteroposteriorly. The posterior wall of the temporal fossa is formed by the squamosal and shows

675 an anterior concavity. Lateral to the posterior wall of the temporal fossa, the supramastoid crest

676 protrudes anteriorly and forms the lateral border of the squamosal fossa.

677 The general features of the temporal fossa of *E. ianitrix* are also observed in *Eubalaena glacialis*

678 and *E. japonica*. *Eubalaena australis* differs in the lack of exposure of the alisphenoid in the

679   temporal fossa at adulthood. In the Pliocene *Eubalaena* sp. from Tuscany (Bisconti, 2002) and

680   *Eubalaena shinshuensis* (Kimura, 2009) the digit-like projection of the anterodorsal portion of the

681   squamosal is absent. In *Balaenula* the posterior apex of the lambdoid crest is located much more

682   anteriorly than in any species belonging to *Eubalaena*, *Balaena* and *Balaenella* and this makes its

683   temporal fossa anteroposteriorly smaller; moreover, in *Balaenula astensis* the posterior wall of the

684   temporal fossa is mainly flat along the dorsoventral axis (Bisconti, 2000, 2003).

685

686   *Palatine.* The palatine is almost rectangular in ventral view (Fig. 10). It is an elongated bone that

687   is anteriorly in contact with the maxilla and posteriorly with the pterygoid. As typically observed

688   in Balaenidae, the palatine is ventrally superimposed on the ventral lamina of the pterygoid that

689   appears, in ventral view, as a small stripe of bone close to the posterior limit of the skull. The

690   ventral surface of the palatine is almost flat. The longitudinal axis of the palatine diverges from

691   the anteroposterior axis of the skull posteriorly as the posterior ends of the palatines are not in

692   contact posteriorly. The lateral lamina of the palatine ascends and contacts the squamosal, the

693   alisphenoid and the frontal.

694   The relationships of the palatine observed in *E. ianitrix* are not different from those that can be

695   observed or inferred in other living and fossil Balaenidae for which information about this bone is

696   available.

697

698   *Pterygoid.* Following Churchill *et al.* (2012), Bisconti (2000, 2005a) and Fraser & Purves (1960),

699   in Balaenidae the pterygoid appears as a small stripe of bone in ventral view. This stripe of bone

700   represents the lateral lamina of the pterygoid that is transversely elongated and approaches the

701   posterior-most border of the skull in lateral view. The pterygoid is dorsally, anteriorly and

702 posteriorly bordered by the squamosal and anteroventrally by the palatine. The posterior border of

703 the pterygoid and the anterior border of the falciform process of the squamosal contribute to delimit

704 the shape of the foramen ovale (Fig. 10).

705 Apart from *Caperea marginata*, in which the foramen ovale is within the pterygoid, the foramen

706 ovale of other balaenoids is located between the squamosal and the pterygoid. In the living species

707 the foramen ovale extends into a tube formed almost entirely by the squamosal (= infundibulum

708 of Fraser and Purves, 1960). This condition is not observed in *E. ianitrix* where the foramen ovale

709 has an olive-like shape.

710

711 **Body size estimate**

712

713 Two of the chosen methods converge towards a total body length or *c.*6-8 m. The application of

714 equation (1) based on a bizygomatic width of 1660 mm (Table 2) retrieved a total body length of

715 *c.* 13 m; this result is to be corrected by reducing it of 37-to-47%. After the correction, the resulting

716 values are respectively *c.* 8 m and *c.* 7 m.

717 The application of the regression equation (4) based on a supraoccipital length of 560 mm (Table

718 2) found a condylobasal length of *c.* 1.6 m. After having tripled and quadrupled this length, the

719 total body length was estimated between 4.74 and 6.37 m.

720 The application of the equation (2) based on an occipital breadth of 353 mm retrieved a body mass

721 of *c.* 33 t. This value is consistent with weight values obtained by Omura et al. (1958) for the North

722 Pacific right whale (*E. japonica*). We used this body mass estimate in the equation (3) and found

723 a total body length of *c.* 11 m, which is closer to the result obtained from the equation (1) before

724 the correction. It is not clear whether the results of the equation (3) need to be corrected but,

725   following the suggestions of Pyenson & Sponberg (2011), we hypothesize that a correction would

726   be necessary that should be around 40%. If we apply such a correction to the value obtained by

727   the equation (3), we find a total body length of *c.* 6.6 m that is very close to the higher results of

728   the equations (1) and (4). If we accept a total body length between 6 and 7 m then we need to apply

729   a roughly similar correction to the estimated body weight. If we reduce the estimated body weight

730   of 40% then we obtain an estimated body weight of 19.8 t.

731   We therefore estimate the total body length of *Eubalaena ianitrix* between 6 and 7 m, with a body

732   mass of *c.* 20 t.

733

734   **Phylogeny**

735

736   *Overview*

737   The phylogenetic analysis resulted in the single most parsimonious cladogram shown in Fig. 12 .

738   Tree statistics are provided in the corresponding caption. Our results confirm the monophyly of

739   Mysticeti, Chaeomysticeti and Balaenomorpha. The sister-group of Balaenomorpha is the

740   monophyletic Eomysticetidae (here represented by *Eomysticetus whitmorei*, *Tokaraia kauaeroa*

741   and *Yamatocetus canaliculatus*). Balaenomorpha is then subdivided into two sister-groups:

742   Balaenoidea and Thalassotherii (including Balaenopteridae, Eschrichtiidae, Cetotheriidae and

743   basal thalassotherian taxa including *Cophocetus*, *Aglaocetus*, *Parietobalaena*, *Isanacetus*,

744   *Uranocetus*, *Pelocetus* and *Diorocetus*). As such, the present results confirm the monophyly of

745   Balaenopteroidea (including Balaenopteridae and Eschrichtiidae) and Cetotheriidae (here

746   including *Mixocetus*, *Herentalia*, *Piscobalaena*, *Herpetocetus* and *Tranatocetus*). *Tranatocetus*

747   *argillarius* is nested here among Cetotheriidae. Although this may be due to our limited sample of

748 Cetotheriidae and related taxa, we are unable to support the monophyly of Tranatocetidae (as

749 proposed by Gol'din & Steeman, 2015), considering that *T. argillarius* (the only nominal

750 Tranatocetidae taxon included in our analysis) falls within Cetotheriidae. Morphological support

751 to Mysticeti, Chaeomysticeti, Balaenomorpha, Thalassotherii, Balaenopteroidea, Cetotheriidae

752 and basal thalassotherian taxa is provided in the Supplementary Information published in the

753 website of the journal.

754 Most surprising are the position of *Morenocetus parvus* (that will be discussed in the next

755 paragraph) and the sister-group relationships within Thalassotherii. Among Thalassotherii, four

756 monophyletic groups of family-level rank are recognized: Balaenopteridae, Eschrichtiidae,

757 Cetotheriidae and a clade including what Bisconti et al. (2013) called basal thalassotherian taxa.

758 Eschrichtiidae is the sister-group of Balaenopteridae and both form the monophyletic

759 Balaenopteroidea. Balaenopteroidea is the sister-group of a large clade including *Titanocetus*

760 *sammarinensis*, Cetotheriidae and basal thalassotherian taxa. *Ti. sammarinensis* is, in its turn, the

761 sister-group of Cetotheriidae and basal thalassotherian taxa.

762

763 *Relationships of Balaenoidea and morphological supports to nodes*

764 Our results support the monophyly of Balaenoidea with a noticeable difference with respect to

765 previously published literature (Cabrera, 1926; Bisconti, 2005; Churchill et al., 2011):

766 *Morenocetus parvus* falls outside Balaenidae + Neobalaenidae and represents the sister-group of

767 both families.

768 Nine synapomorphies support the monophyly of Balaenoidea. Three of them depends on the

769 structure of the skull: characters 37 (short exposure of interorbital region of the frontal because of

770 superimposition by the parietal), 54 (massive elongation of supraoccipital), and 55 (supraoccipital

771 is superimposed onto the interorbital region of the frontal). Moreover, character 47 (squamosal

772 dorsoventrally elongated) is also an exclusive synapomorphy of this clade.

773 Seventeen synapomorphies support the monophyly of Neobalaenidae + Balaenidae to the

774 exclusion of *Morenocetus parvus*. Three of them are unambiguous: characters 81 (low tympanic

775 cavity), 82 (dorsoventrally compressed tympanic bulla), and 83 (enlargement of epitympanic

776 hiatus). Characters 11 (rostrum highly arched), 84 (anteroposteriorly short anterolateral lobe of

777 tympanic bulla), 92 (dorsal exposure of mandibular condyle), 95 (dorsoventral arc of dentary along

778 the whole length of the bone), and 101 (cervical vertebrae fused) represent additional ambiguous

779 synapomorphies of the clade. Neobalaenidae (including *Caperea* and *Miocaperea*) is the sister-

780 group of Balaenidae (here including *Balaena, Balaenella, Balaenula* and *Eubalaena*). The

781 monophyly of Neobalaenidae is supported by 4 synapomorphies including a reversal in character

782 122 (complete infundibulum). Characters 50 (presence of squamosal cleft) and 75 (exposure of

783 posterior process of petrotympanics in the lateral view of the skull) are ambiguous synapomorphies

784 as these characters (in different ways) are observed in Balaenopteridae and Cetotheriidae,

785 presumably as a result of convergent evolution.

786 Four unambiguous synapomorphies support the monophyly of Balaenidae: characters 64 (massive

787 elongation of palatine posteriorly), 65 (posterior placement of pterygoid), 86 (sharply defined

788 groove for mylohyoidal muscle), and 122 (foramen ovale with incomplete infundibulum). Three

789 additional ambiguous synapomorphies are detected: characters 12 (transverse compression of

790 maxilla), 74 (long and thick roof of stylomastoid fossa), and 97 (strong anterior torsion of dentary).

791 Balaenidae is subdivided into two clades: one including *Balaena* and *Balaenella* and the other

792 including *Balaenula* and *Eubalaena*. The inclusion of *Balaenella brachyrhynus* within *Balaena*

793 casts some taxonomic problems as it either makes *Balaena* paraphyletic or suggests inclusion of

794 *Balaenella* within *Balaena*. *Balaenella brachyrhynus* and *Balaena montalionis* share an anteriorly

795 narrowed supraoccipital and a supraoccipital with transversely short anterior border; these

796 character states support their sister-group relationship. Unfortunately, a clear illustration of the

797 dorsal view of *Balaena ricei* is not available and it is difficult to understand whether this species

798 is really more closely related to *Balaena montalionis* and *Balaenella brachyrhynus* or to *Balaena*

799 *mysticetus*. From our results, *B. mysticetus* represents a separate lineage that diverged before the

800 other *Balaena*-like taxa (*B. ricei*, *B. montalionis* and *Balaenella*). A low number of

801 synapomorphies support the monophyly of the clade including *Balaena* and *Balaenella*. These

802 include the following two unambiguous synapomorphies: characters 116 (transverse compression

803 of anterior supraoccipital) and 120 (lateral projection of zygomatic process of the squamosal).

804 Additionally, two ambiguous synapomorphies are also found to support this clade; these include

805 characters 126 (posterior orientation of dorsoventrally developed squamosal body) and 132 (crest

806 present at parietal-squamosal suture). The sister-group relationship of *Balaena montalionis* and

807 *Balaenella brachyrhynus* is supported by one unambiguous synapomorphy (character 117: squared

808 anterior border of supraoccipital) and one ambiguous synapomorphy (character 118: short anterior

809 border of supraoccipital).

810

811

812 *Relationships of* Eubalaena

813 Confirming previously published hypotheses (Bisconti, 2000, 2005a; Churchill et al., 2012), our

814 analysis resulted in the monophyly of a clade including *Balaenula* and *Eubalaena* (Fig. 12). The

815 clade including *Eubalaena* and *Balaenula* is the sister-group to the *Balaena + Balaenella* clade.

816 *Balaenula* is the sister-group of *Eubalaena*. Three unambiguous and one ambiguous

817 synapomorphies support this clade. The unambiguous synapomorphies include characters 123

818 (transverse orientation of supraorbital process of the frontal in lateral view), 129 (curvature of the

819 rostrum with horizontal proximal part), and 130 (concavity on the anterior border of nasal).

820 Character 118 (transversely wide anterior border of supraoccipital) was also found to support this

821 clade (ambiguous synapomorphy).

822 *Eubalaena shinshuensis* is the first *Eubalaena* species to branch; the *Eubalaena* sp. from the Late

823 Pliocene of Tuscany is the sister-group of the living *Eubalaena* species + *E. ianitrix* and its

824 inclusion on a separate ramus suggests that it could be a different *Eubalaena* species of its own.

825 *Eubalaena japonica* and *E. australis* branch before *E. ianitrix* and *E. glacialis*, the two latter being

826 sister-groups.

827 Only one unambiguous synapomorphy was found to support the monophyly of the right whale

828 genus *Eubalaena*; character 115 (presence of a dome on the supraoccipital). *Eubalaena*

829 *shinshuensis* from the Messinian of Japan was found to be the earliest-diverging right whale

830 species of the genus; the Pliocene *Eubalaena* sp. from Tuscany is the sister-group of the living

831 *Eubalaena* species + *E. ianitrix*. The monophyly of the *Eubalaena* sp. from Tuscany and the

832 crownward *Eubalaena* species was supported by one unambiguous synapomorphy (character 127:

833 squared exoccipital in lateral view) and one ambiguous synapomorphy (character 126: vertical

834 orientation of squamosal body).

835 The clade including the living *Eubalaena* species and *E. ianitrix* is supported by 5 unambiguous

836 synapomorphies (125: parietal-frontal suture with distinctive anteroventral corner; 131: short

837 nasals; 133: parietal spreads on the supraorbital process of the frontal; 140: presence of vascular

838 groove on posterior part of pars cochlearis; and 141: evident pyramidal process posterior to

839 perilymphatic foramen) and 8 ambiguous synapomorphies (114: sagittal concavity on

840 supraoccipital; 134: anterior protrusion of parietal-squamosal suture; 135: prismatic posterior

841 process of petrosal; 138: transversely elongated pars cochlearis; 143: long transverse process of

842 the atlas; 146: highly concave anterior and posterior borders of humerus; 147: globular humeral

843 head; 150: superior corner of olecranon reduced-to-absent; and 151: reduced-to-absent coracoid

844 process in scapula.

845 *Eubalaena australis* was found to be more closely related to *E. ianitrix + E. glacialis* than *E.*

846 *japonica*. The sister-group relationship of *E. glacialis* with *E. ianitrix + E. glacialis* was supported

847 by two unambiguous synapomorphies: characters 139 (crista transversa exits from internal

848 acoustic meatus) and 152 (transverse orientation of tyrohyoidal processes). It is noticeable that

849 none of these characters is preserved in the holotype of *E. ianitrix* and the placement of this species

850 in this precise position in the cladogram relies on ACCTRAN optimization of the morphological

851 transformations operated by TNT. The monophyly of the clade *Eubalaena ianitrix + E. glacialis*

852 is supported by a single ambiguous synapomorphy: character 121 (presence of pterygoid in

853 temporal fossa).

854

855 *Stratigraphic Consistency Index*

856 The calculus of the Stratigraphic Consistency Index shows that the degree of agreement of the

857 branching pattern with the stratigraphic occurrence of the taxa is exceptionally high. The SCI

858 depends on (1) the number of well-resolved nodes and (2) the number of stratigraphically

859 consistent nodes. In the hypothesis of phylogeny presented in this paper, the maximum number of

860 nodes is 40 (number of OTUs minus 2) and the number of stratigraphically consistent nodes is 33.

861 The SCI is thus 0.825.

862

863   *Divergence dates of balaenoid clades*

864   In Fig. 14 the hypothesis of phylogeny for Balaenoidea proposed in the present paper is plotted

865   against the stratigraphic age of the included OTUs. In the Figure, branch lengths are inferred from

866   the phylogenetic relationships of the taxa and from the stratigraphic ages of the representative

867   fossil record of each OTU.

868   The age of *Miocaperea pulchra* suggests that the origin of the clade including Balaenidae +

869   Neobalaenidae is older than Tortonian (early Late Miocene). Unfortunately, given that

870   *Morenocetus parvus* falls outside Neobalaenidae + Balaenidae, it is not possible to be sure about

871   the precise age of origin of these families. Indeed, as the stratigraphic occurrence of *M. parvus* is

872   limited to the Burdigalian (late Early Miocene), the age of origin of Neobalaenidae and Balaenidae

873   may be constrained to a time interval between Burdigalian and Tortonian.

874   The fossil record of *Balaena*-like species does not extend before Zanclean (Early Pliocene). The

875   stratigraphic occurrences of *Balena montalionis*, *B. ricei* and *Balaenella brachyrhynus* suggest

876   that an expansion of the paleobiogeographic range of *Balaena*-like taxa was attained during the

877   earliest part of the Pliocene with invasion of Mediterranean, North Atlantic and North Sea. The

878   sister-group relationship of *Balaena mysticetus* and the other *Balaena*-like taxa suggest that the

879   direct ancestor of the living bowhead whale originated around the Zanclean or slightly earlier and

880   possibly quickly invaded the Arctic region, leaving us more limited possibilities to find fossil

881   records relevant for the morphological transition towards the extant species.

882   The stratigraphic age of *Eubalaena shinshuensis* is the most crucial point in the present

883   reconstruction of the divergence dates of balaenoid taxa. In fact, as the occurrence of this species

884   is from the Messinian, the origin of the whole *Balaenula + Eubalaena* clade must be traced back

885   to at least the latest Miocene. This means that the separation of the living right whales from their

886 closest living relative (i.e., *Balaena mysticetus*) is from 7-to-5.4 million years ago which

887 significantly increases the hypothesized divergence date based on McLeod et al. (1993) and

888 reduces to one-third of the hypothesized divergence date based on Bisconti (2005b) and Santangelo

889 et al. (2005). The impact of this new divergence date on the reconstruction of the demographic

890 history of the right whales based on genetic measures of diversity will be analysed elsewhere.

891 As far as the origins of the living *Eubalaena* species is concerned, the Messinian age of *E.*

892 *shinshuensis* suggests that the origin of the genus *Eubalaena* should be found at least in the latest

893 Miocene. The stratigraphic occurrences of the *Eubalaena* sp. from Tuscany and *E. ianitrix*

894 constrain the origin of the living right whale species to at least the Piacenzian. Therefore, we

895 estimate that the modern *Eubalaena* species originated in a period between 3.5 and 2.6 Ma. As we

896 will show in another paragraph, it is more difficult to determine a chronological placement for the

897 origin of the northern right whale *E. glacialis* because the origin of this species could be due to a

898 process of phyletic transformation from *E. ianitrix*, occurring in a time interval ranging from the

899 Piacenzian to the Pleistocene.

900 In summary, the stratigraphic distribution of the main evolutionary events of Balaenoidea are

901 presented in Fig. 13. Following our phylogenetic analysis and the computation of stratigraphic

902 ages of the included OTUs, the origin of Balaenoidea should be traced at least as far as the

903 Burdigalian (age of *Morenocetus parvus*). The origin of the living families (Neobalaenidae and

904 Balaenidae) occurred before the Tortonian (age of *Miocaperea pulchra*). The splitting between the

905 *Balaena*-like and the *Balaenula + Eubalaena* clades occurred before the Messinian (age of

906 *Eubalaena shinshuensis*). The origin of the modern *Eubalaena* radiation (including *E. ianitrix*)

907 dates at least from the Piacenzian. The separation between the living right whale species and their

908 extant relative (*Balaena*) dates at least from the earliest Messinian (*c.* 7 Ma).

909

910   **Discussion**

911

912   *Phylogeny: Relationships of Balaenidae*

913   Phylogenetic analyses of Balaenidae were published by several authors in the last 25 years.

914   McLeod et al. (1993) were the first to publish a phylogenetic tree based on manual manipulation

915   of morphological character states. They found a monophyletic Balaenoidea and a sister group

916   relationship between Neobalaenidae and a clade formed by Balaenidae and Eschrichtiidae. The

917   sister-group relationship of Balaenidae and Eschrichtiidae was not confirmed by subsequent

918   phylogenetic works.

919   Bisconti (2000) performed the first computer-assisted cladistic analysis of Balaenidae, retrieving

920   a monophyletic Balaenoidea and a monophyletic Balaenidae. Within Balaenidae, Bisconti (2000)

921   found two different clades: one including the genus *Balaena* and the other including *Eubalaena*,

922   *Balaenula* and *Morenocetus*. After a substantial re-discussion of the fossil record of Balaenidae

923   (Bisconti, 2003) and of previously published phylogenetic analyses, Bisconti (2005a) published a

924   new phylogenetic analysis resulting in a monophyletic Balaenoidea and a monophyletic

925   Balaenidae; two clades were recovered in Balaenidae: one included *Morenocetus*, *Balaenella* and

926   *Balaena* and the other included *Eubalaena* and *Balaenula*. These finds were substantially

927   confirmed by Churchill et al. (2012) after an extensive reanalysis of the morphological evidence

928   of the phylogeny of Balaenidae.

929   Numerous other works on the phylogeny of mysticetes were published in the last decades that

930   included balaenids, but not explicitly focused on Balaenidae. However, it is important to consider

931   these works as they provide information about the sister-group relationships of Balaenidae and

932   other mysticete taxa. While most of the morphology-based works agree that Balaenidae and

933   Neobalaenidae are sister-groups (Bisconti, 2015 and literature therein; Boessenecker & Fordyce,

934   2016), several recent papers did not support the monophyly of Balaenoidea with Neobalaenidae as

935   sister group of Balaenopteroidea (see Gol'din et al., 2014 and literature therein) or as part of

936   Cetotheriidae (e.g., Marx & Fordyce, 2015 and literature therein). The placement of *Caperea*

937   *marginata* and *Miocaperea pulchra* within Cetotheriidae depended upon peculiar treatments of

938   some characters related to the shape and orientation of the squamosal, the elongation of the

939   supraoccipital and the reduction of the ascending process of the maxilla. Criticisms to this

940   approach were published by El Adli et al. (2014) and Bisconti (2015) suggesting that the Marx &

941   Fordyce (2015) dataset should be revised. Marx & Fordyce (2016) provided a subsequent version

942   of such a dataset that shows substantially the same characteristics, as it does not include character

943   states describing the topological relationships of the bones forming the skull vault in Balaenidae

944   and   Neobalaenidae.   The   proposed   sister-group   relationship   of   Neobalaenidae   and

945   Balaenopteroidea + Cetotheriidae depends on (1) inclusion of molecular data or (2) emphasis on

946   rorqual-like characters observed in *Caperea marginata* (i.e., long forelimb, presence of dorsal fin,

947   and presence of ventral throat grooves).

948   The problem of using molecular data to infer the phylogenetic relationships of clades mainly

949   formed by fossil taxa was addressed by several authors and this is the precise case of mysticetes

950   where most of the described species are now extinct and cannot be used for DNA sequencing and

951   analysis. Even if molecular analyses may include thousands of character states (base pairs from

952   DNA sequences), the lack of data from most of the taxa belonging into the clade may be a serious

953   problem as an enormous number of character states cannot be scored and must be inferred by the

954   computer program used for the analysis. The accuracy of phylogenetic reconstructions based on

955 molecular data for clades mainly formed by extinct taxa tends to be lower than that based on

956 morphological data (Heath et al., 2008; Wagner, 2000). This suggests that emphasis should be

957 given to morphological rather than molecular data in the inference of the phylogeny of mysticetes.

958 Aside from that, it must be said that taxonomic uncertainties, problems with character descriptions

959 and coding, and the discovery of large amounts of homoplasy in morphological datasets have

960 plagued morphological attempts to infer phylogenetic relationships in mysticetes in the last twenty

961 years (Deméré et al., 2005; Bisconti, 2007). Our effort to reduce dataset homoplasy was successful

962 only in part. In fact, after the exclusion of evident homoplastic characters from our morphological

963 dataset, the number of usable character states dropped down and our morphological evidence could

964 provide only strong support for only some clades. Most of the species-level sister group

965 relationships are thus supported by reduced numbers of synapomorphies. In this sense, what we

966 observe in balaenid phylogenetics resembles what was observed in complicated analyses of

967 evolutionary radiations occurring in relatively recent times (e.g., cichlid fishes and hominins; e.g.,

968 Seehausen, 2006; Haile-Selassie et al., 2016) with the important difference that the evolutionary

969 radiation of Balaenidae occurred in a longer time interval. However, studies of DNA substitution

970 rates interestingly showed that mysticete DNA evolves much more slowly than that of other

971 mammals (Rooney et al., 2001); therefore, only limited morphological change should be expected

972 to occur in this group in the last few million years. This expectation is somewhat confirmed by the

973 substantial stasis detected in the last 10 million years of neobalaenid evolution (Bisconti, 2012)

974 and by the small amount of morphological diversity observed in Balaenidae as discussed in this

975 work. The reasons of the slow evolutionary pace in Balaenidae are not completely understood; one

976 character that could be correlated is the evolution of increased individual longevity, demonstrated

977   to be linked to DNA preservation (Jackson et al., 2009; Keane et al., 2015), which, in its turn,

978   should reduce the accumulation of mutations preventing the evolution of phenotypic diversity.

979

980   *Phylogeny: intra-family relationships within Balaenidae*

981   Published studies specifically directed at discovering phylogenetic relationships of Balaenidae

982   recently converged towards the subdivision of this family into two sub-clades: a clade including

983   *Balaena* and *Balaenella* and a clade including *Balaenula* and *Eubalaena*. These two groups are

984   well supported by morphological characters and correspond to two different skull structures (as

985   evidenced by Miller, 1923; Kellogg, 1928; McLeod et al., 1993; Bisconti, 2005a).

986   The contribution of the postcranial skeleton to the support for these clades is rather scanty but, for

987   the first time, we detected that: (1) the dorsal transverse process of the atlas is dorsoventrally

988   enlarged in *Eubalaena* and reduced in *Balaena* (including *B. mysticetus* and *B. ricei*), (2) the

989   ventral transverse process of the atlas is long and forms a ventral corner in *Balaena* but is short

990   and squared in *Eubalaena*, (3) the humerus is long and slender in *Balaena* while in *Eubalaena* it

991   is shorter and with a more globular head, and (4) the dorsal corner of the olecranon process of the

992   ulna is conspicuous in *Balaena* but reduced to absent in *Eubalaena*.

993   The four characters outlined above could be useful to suggest phylogenetic and taxonomic

994   affinities of fossils of uncertain position because of their poor preservation. This is the case of a

995   number of partial skeletons from the Pliocene of Italy (Bisconti, 2003; Chicchi & Bisconti, 2014;

996   Cioppi, 2014; Bisconti & Francou, 2014; Manganelli & Benocci, 2014; Sarti & Lanzetti, 2014)

997   that should be reassessed based on this new evidence.

998   As mentioned above, the sister-group relationship of *Balaena montalionis* and *Balaenella*

999   *brachyrhynus* raises particular problems as the inclusion of *Balaenella* within *Balaena* would

1000   either make the latter paraphyletic, or would imply the assignment of *Balaenella* to *Balaena*.

1001   However, we feel that it is premature to choose one of the above options, as some morphological

1002   data from *Balaena ricei* were not available for this study (i.e., precise sutural pattern between

1003   parietal and frontal and between parietal and squamosal, and shape of the anterior end of the

1004   supraoccipital); this makes relationships within the *Balaena*-like subclade still biased by some

1005   uncertainty. However, the close relationship of *B. montalionis* and *B.lla brachyrhynus* seems well

1006   supported by the shared squared anterior border of the supraoccipital and the transverse

1007   compression observed in the anterior half of the lateral borders of the supraoccipital. The point,

1008   here, consists in understanding if *Balaena ricei* is more closely related to *Balaena mysticetus* or to

1009   the *B. montalionis* + *B.lla brachyrhynus* pair; more data are needed about the morphology of *B.*

1010   *ricei* to solve this question.

1011   Among right whales, *Eubalaena shinshuensis* is the first to branch off, due to the primitive sutural

1012   pattern observed in the skull of this Messinian species; the following branch is occupied by the

1013   Piacenzian *Eubalaena* sp. from Tuscany, due to the plesiomorphic parietal-squamosal suture and

1014   to a peculiar supraoccipital morphology. More interesting are the relationships of the living

1015   *Eubalaena* species and *E. ianitrix*. From our work, *E. japonica* is the earliest-diverging species

1016   among the living right whales, with *E. australis* and *E. glacialis* more closely related to each other.

1017   This result contradicts molecular studies that suggested that *E. australis* diverged earlier and that

1018   *E. glacialis* and *E. japonica* are sister-groups (e.g., Gaines et al., 2005; Rosenbaum et al., 2000).

1019   Also the DNA-based phylogeny of species of lices parasitizing living *Eubalaena* species lends

1020   support to the molecular hypothesis of relationships for right whales (e.g., Kaliszewska et al.,

1021   2005) thus suggesting that *E. glacialis* is the earliest-diverging *Eubalaena* species. However, these

1022   analyses did not include data from fossil right whales such as *E. shinshuensis*, *E. ianitrix*, and the

1023   *Eubalaena* sp. from Tuscany and did not take into account the fossil histories of the different lice

1024   species; therefore, they could be unable to retrieve correct results (in accordance with Heath et al.,

1025   2008; Wagner, 2000). Moreover, assuming an early branching of *E. glacialis* in the phylogeny of

1026   the living right whales implies that reticulate biogeographic histories have occurred between the

1027   southern and the North Pacific *Eubalaena* species to account for the peculiar genetic patterns

1028   observed in cyamid lices (Kaliszewska et al., 2005).

1029

1030   *Divergences of the living right whale species*

1031   Divergence ages of living balaenid species are important for the reconstructions of the

1032   demographic histories of these taxa in the context of conservation biology. Divergence dates are

1033   used in equations dealing with the genetic diversity of the living populations to assess whether

1034   living species suffered of genetic bottlenecks due to environmental change or human impact (e.g.,

1035   Rosenbaum et al., 2001). Fossil calibrations of divergence dates are necessary to constrain the pace

1036   of molecular clocks in order to get correct results in terms of assessments of genetic diversity and

1037   evolution (Quental & Marshall, 2010).

1038   Several works have provided estimates of divergence ages of balaenid species. McLeod et al.

1039   (1993) suggested a separation date between *Eubalaena* and *Balaena* of *c.* 4.5 Ma based on analysis

1040   of the balaenid fossil record. This assessment was used by Rosenbaum et al. (2001) to analyse the

1041   genetic diversity of the living bowhead whale, *Balaena mysticetus*, with the conclusion that this

1042   species did not suffer of population bottlenecks due to human whaling activities. Bisconti (2005b)

1043   and Santangelo et al. (2005) questioned this conclusion based on the phylogenetic analysis

1044   provided by Bisconti (2005a); the latter opened the possibility that the divergence between

1045   *Eubalaena* and *Balaena* occurred in the Early Miocene. This conclusion resulted from the

1046   placement of *Morenocetus parvus* as sister-group of the *Balaena*-like subclade to the exclusion of

1047   the *Balaenula + Eubalaena* subclade (Bisconti 2005a) thus providing a divergence date of *Balaena*

1048   and *Eubalaena* of more than 20 Ma.

1049   Subsequent analyses did not confirm this result as molecule-based and morphology-based works

1050   suggested later divergence dates (e.g., Sasaki et al., 2007; Churchill et al., 2011) and placed the

1051   divergence of *Balaena* and *Eubalaena* in a time interval ranging from *c.* 4 to *c.* 7 Ma. The

1052   phylogenetic analysis of *Cyamus* lices confirms a divergence at *c.* 6.6 Ma for the living right whale

1053   and bowhead whale species (Kaliszewska et al., 2005).

1054   The phylogenetic analysis of the present work (Figs 12 and14) reinforces a minimum late Miocene

1055   divergence (Messinian: *c.* 7-5.4 Ma) based on the age of the earliest diverging *Eubalaena* species

1056   (i.e., *E. shinshuensis*). In fact, an earlier divergence age is not unlikely, considering that (1) the

1057   separation between Balaenidae and Neobalaenidae dates from at least the Tortonian (*c.* 10 Ma)

1058   and (2) the separation of the *Balaena*-like subclade from the *Balaenula + Eubalaena* subclade is

1059   deep in time and originates from the very origin of Balaenidae (Bisconti, 2005a; Churchill et al.,

1060   2011; this work).

1061   How the reconstructions of the demographic histories of balaenids will be impacted by a Late

1062   Miocene age of divergence between *Eubalaena* and *Balaena* is outside the scopes of the present

1063   paper. However, we suggest here that the past estimates of genetic diversity in right and bowhead

1064   whale populations should be considered with caution as those were based on underestimated

1065   (McLeod et al., 1993) or overestimated (Bisconti, 2005b; Santangelo et al., 2005) divergence ages.

1066

1067   *Possible ancestor-descendant relationships between* Eubalaena ianitrix *and* Eubalaena glacialis

1068   There is not a commonly accepted method to infer ancestor-descendant relationships (ADRs) in

1069   phylogenetics as it is supposed that only in exceptional cases such a relationship can be detected

1070 in the fossil record (Paul, 1992). The most usual recommendation to those who try to recover ADR

1071 from the fossil record consists in being sure that a reasonably complete sample is available for the

1072 past diversity of the investigated group. While it is certain that this is not the case for fossil

1073 cetaceans, some attempts to reconstruct ADRs in this order were attempted in the past with a

1074 diversified array of methods.

1075 Uhen & Gingerich (2001) provided an ADR for *Chrysocetus healyorum* and Neoceti (Mysticeti +

1076 Odontoceti). They used a stratocladistic approach in three steps: (1) they performed a traditional

1077 computer-assisted, morphology-based cladistics analysis retrieving a set of resulting cladograms;

1078 (2) they added a stratigraphic character and manipulated the initial hypothesis of relationships by

1079 hand in order to explore whether *C. healyorum* could be the direct ancestor of Neoceti; (3) they

1080 calculated a new set of cladograms via a computer-assisted algorithm. They found one most

1081 parsimonious tree in which *C. healyorum* was placed as direct ancestor of Neoceti. In the

1082 subsequent discussion, they suggested that newly discovered advanced archaeocetes taxa could fit

1083 the ancestor position for Neoceti in a better way than *C. healyorum* thus giving this taxon a

1084 temporary ancestor status.

1085 More recently, Tsai & Fordyce (2015) suggested an ADR for *Miocaperea pulchra* and *Caperea*

1086 *marginata* based on a combination of cladistic analysis of traditional OTUs + juvenile individuals

1087 of *C. marginata* and by providing a discussion on the impact of the morphology of juvenile

1088 characters in phylogeny reconstruction.

1089 All of these methods have their own merits and shortcuts; Uhen & Gingerich (2001) realized a

1090 systematized search for the most parsimonious solutions but their results were limited by

1091 uncertainties about the completeness of the relevant fossil record; Tsai & Fordyce (2015) used data

1092 from a hotly debated source of data (i.e., juvenile and embryonic specimens) (e.g., Hall, 1996 and

1093   literature therein). Apart from that, however, the search for ADRs is always worth doing, as it

1094   potentially gives information on natural evolutionary processes.

1095   Here, we suggest that an ADR should be proposed for the *Eubalaena ianitrix* and *Eubalaena*

1096   *glacialis* species pair. We support our hypothesis of relationships based on what follows:

1097   (1) *E. glacialis* and *E. ianitrix* are phylogenetically more closely related than all the other

1098   species belonging to *Eubalaena*; they share one peculiar synapomorphy that is not

1099   observed in any other *Eubalaena* species (i.e., presence of the pterygoid in the temporal

1100   fossa).

1101   (2) Molecular studies suggest that the branch of *E. glacialis* has been separated from the other

1102   living right whale species for a long time (up to 3 million years). This long time interval

1103   excludes the possibility of an arrival in the North Atlantic due to a recent invasion from the

1104   North Pacific or the southern right whale species (Kaliszewska et al., 2005). Thus, it is

1105   highly likely that *E. glacialis* originated in that portion of the northern hemisphere that

1106   includes the North Atlantic and the North Sea.

1107   (3) *E. glacialis* and *E. ianitrix* share part of their geographic distribution. Even if only one

1108   specimen of *E. ianitrix* is known up to now, its geographic occurrence is included within

1109   the geographic range of *E. glacialis*.

1110   (4) The geographic area that encompasses the distribution of *E. ianitrix* and *E. glacialis*

1111   underwent extensive environmental change during the past 1.5 million years (Zachos et al.,

1112   2001), supporting the hypothesis that selective regimes could have been active there

1113   implying phenotypic evolution in previously established populations. In particular, the

1114   temperature decline observed in the whole northern hemisphere during the Pleistocene

1115   could have been the driver of organismal responses that can be described (in part, at least)

1116   by the Bergmann's rule (i.e., increasing body size).

1117   (5) Assuming a species longevity of 2 million years (Fordyce & de Muizon, 2001; Steeman et

1118   al., 2009), and hypothesizing that *Eubalaena glacialis* became a well-defined species

1119   around the Pliocene-Pleistocene boundary, there may be a time interval in which *E. ianitrix*

1120   and the earliest individuals of *E. glacialis* co-occurred in the same area where the

1121   morphological transition happened.

1122   (6) Bearing in mind the paleoenvironmental changes that occurred in the northern hemisphere

1123   from the earliest Pleistocene (*c.* 2.6 Ma) through most of the epoch, a phyletic

1124   transformation of a previously established population of right whale into a more

1125   phenotypically-optimized species is a reasonable hypothesis.

1126   (7) From a skeletal morphology perspective, if a phyletic transformation of *E. ianitrix* into *E.*

1127   *glacialis* occurred, then it involved only: (1) massive size increase at adulthood enabling

1128   the extant *E. glacialis* to reach more than 20 m in length at maturity (Tomilin, 1967) against

1129   the *c.* 7 m of *E. ianitrix* (consistent with Bergmann's rule in a colder environment), (2)

1130   possible allometric adjustments of bone proportions (this is a direct consequence of point

1131   1), (3) loss of the crest at the parietal-squamosal-supraoccipital suture, and (4) change in

1132   the orientation of the posteromedial corner of the palatine. The crest at parietal-squamosal-

1133   supraoccipital suture appears to have been lost in the common ancestor of *E. glacialis* + *E.*

1134   *ianitrix* + *E. japonica* + *E. australis* clade and its presence in *E. ianitrix* is to be interpreted

1135   as a reversal to a plesiomorphic condition. The same applies to the protrusion of the

1136   posteromedial corner of the palatine. The recurrent evolution of these two characters

1137   suggests that some homoplasy occurred in the above clade in the last few million years.

1138   (8) Current genetic evidence supports the view that three distinct species of right whales

1139   inhabit three different ocean basins (Malik et al., 2000; Rosenbaum et al., 2001):

1140   *Eubalaena glacialis* in the North Atlantic and adjacent waters, *E. japonica* in the North

1141   Pacific, and *E. australis* in the Southern Ocean. Balaenoid whales perform a particular

1142   feeding behavior directed at capturing calanoid copepods; this feeding behavior is known

1143   as continuous ram feeing (Sanderson & Wassersug, 1993) or skim feeding (Pivorunas,

1144   1979). In the northern hemisphere, there is a geographic separation between the skim

1145   feeding species: the bowhead whale inhabits Arctic waters, while the right whales inhabit

1146   more temperate waters and the two right whale species of the northern hemisphere are

1147   separated by the Eurasia and thus do not compete for food or reproductive areas. In the

1148   southern hemisphere, the two skim feeding species are geographically separated as the

1149   southern right whale feeds around Antarctica while the pygmy right whale is restricted to

1150   more temperate waters; apparently, there is no competition between these species for food

1151   or reproductive areas. It appears, thus, that only one skim feeding species is "allowed" to

1152   live in a given ocean basin, and we may hypothesize that the pattern was not different in

1153   the past million years. For this reason, we may expect that only one or a few right whale

1154   species occupied a given geographic area in time intervals of *c*. 2 million years (mean

1155   duration of a marine mammal species; see above). This suggests that, paradoxically, the

1156   taxonomic sample of the right whale diversity in the Late Pliocene of the northern

1157   hemisphere is rather complete. This inference is also confirmed by the high value of the

1158   SCI obtained here, suggesting that most of the phylogenetic relationships presented here

1159   can be explained without the need for long ghost lineages. This inference fills the requests

1160   for a dense taxonomic sampling in the taxa under investigation and allows us to give further

1161   support to our hypothesis of ADR for *Eubalaena ianitrix* and *E. glacialis*.

1162   (9) In a way to test the ADR for *Eubalaena ianitrix* and *E. glacialis*, we followed the

1163   stratocladistic approach of Uhen & Gingerich (2001). The taxon x character matrix and the

1164   single most parsimonious tree were taken to MacClade (Maddison & Maddison, 2000).

1165   First, without the addition of a stratigraphic character, the ADR for *E. ianitrix* and *E.*

1166   *glacialis* was demonstrated to increase the tree length of two steps, as compared to the

1167   original tree length with a sister-group relationship. After addition of the stratigraphic

1168   character (see Supplementary Information) and without any other modification of the

1169   topology, the difference in tree length decreased from two steps to one step, meaning that

1170   the sister-group relationship was still the most parsimonious, but that stratigraphic data,

1171   namely the Piacenzian age of *E. ianitrix*, made the difference less significant. Swapping

1172   branches by hand, ADR for *E. ianitrix* and *E. glacialis* was found more parsimonious than

1173   a sister-group relationship only with (1) *E. shinshuensis* being more stemward than

1174   *Balaenula astensis*, and (2) the three extant *Eubalaena* species forming a clade, with *E.*

1175   *ianitrix* as their last common ancestor. The need for such changes in topology may indicate

1176   that *E. ianitrix* is not the ancestor of *E. glacialis*. However, we think that such a pattern is

1177   strongly impacted by the scanty Pliocene balaenid fossil record in some areas (for example

1178   the North Pacific and the Southern Ocean). Pending the future discovery of fossil relatives

1179   of *E. australis* and *E. japonica*, stratocladistic analyses will most likely not be able to

1180   unambiguously discriminate ADR and sister-group relationships for *E. ianitrix* and *E.*

1181   *glacialis*.

1182

1183   **Conclusions**

1184

1185   We re-described specimens previously referred to *'Balaena' belgica* and found what follows.

1186   (1) The cervical complex RBINS M. 881 (IG 8444) that was originally designated as type of

1187   *'Balaena belgica* by Abel (1941) is poorly preserved and does not show diagnostic

1188   characters below the family level; therefore, we assign it to Balaenidae gen. et sp. indet.;

1189   this decision makes *'Balaena' belgica*, and its recombination nomina dubia.

1190   (2) The fragment of maxilla RBINS M. 880 lacks crucial diagnostic characters and cannot be

1191   assigned to any of the described balaenid genera and species; it is therefore assigned to

1192   Balaenidae gen. et sp. indet.

1193   (3) The morphology of the humerus RBINS M. 2280 is closer to that of *Eubalaena glacialis*

1194   as compared to *Balaena mysticetus* in the shape of the articular facet for the olecranon

1195   process of the ulna, in the overall shape of the deltoid tuberosity, and in the shape of the

1196   posterior border of the diaphysis. However, it differs from *E. glacialis* and other extant

1197   *Eubalaena* species in the elongation of the straight posterior border of the diaphysis; it is

1198   therefore assigned to *Eubalaena* sp. indet. This humerus corresponds to a large individual

1199   reaching a total body length over 16.5 m; it represents the first report of a gigantic right

1200   whale in the fossil record of the North Sea.

1201   (4) The neurocranium RBINS M. 879a-f represents the holotype of the new species *Eubalaena*

1202   *ianitrix*. This species is described and analysed into a phylogenetic context. From a

1203   morphological viewpoint, *E. ianitrix* is very close to the northern right whale *E. glacialis*

1204   in having the same sutural pattern in the skull vault and in sharing the presence of pterygoid

1205   in the temporal fossa. From a phylogenetic view, *E. ianitrix* is the sister-group of *E.*

1206   *glacialis*.

1207   (5) Our phylogenetic analysis also retrieved a monophyletic Balaenoidea, with *Morenocetus*

1208   *parvus* as the earliest stem balaenoid taxon, and with Neobalaenidae being the sister-group

1209   of Balaenidae. Two clades are observed within Balaenidae: one including *Balaena*-like

1210   taxa (genera *Balaena* and *Balaenella*) and the other including *Balaenula* and *Eubalaena*.

1211   The Messinian *E. shinshuensis* is the earliest diverging *Eubalaena* species; the *Eubalaena*

1212   sp. from Tuscany is the sister-group of a clade including all the living *Eubalaena* species

1213   and *E. ianitrix*.

1214   (6) The separation of *Eubalaena* from *Balaena* is estimated to have occurred around 7 Ma

1215   (minimum age). The origins of the living right whale species should be chronologically

1216   constrained to the Piacenzian (Late Pliocene: at least between 3.6 and 2.6 ma). Judging

1217   from supporting synapomorphies, stratigraphic ranges and ecological requirements, it is

1218   suggested that *Eubalaena ianitrix* is the direct ancestor of *E. glacialis*, the latter is proposed

1219   to have evolved via phyletic transformation, through body size increase and allometric

1220   adjustments during the temperature decline of the latest Pliocene and Pleistocene.

1221

1222

1223

1224   *Acknowledgments*

1225   The authors wish to thank Annelise Folie, Alain Drèze and Cécilia Cousin (all at RBINS, Brussels)

1226   for providing access to the specimens and for assisting in the transport of these heavy bones; Marc

1227   Spolspoel for his help when taking photos of part of the specimens illustrated here. Many thanks

1228   are due to Richard Monk, Eric Brothers, Eileen Westwig, Maria Dickson, and Nancy Simmons

1229   (all at AMNH, New York), Graham and Margaret Avery and Leonard Compagno (all at IZIKO,

1230 Cape Town), Reinier Van Zelst, John De Vos, Steven Van Der Mije and Wendy Van Bohemen

1231 (all at Naturalis, Rotterdam) for granting access to specimens under their care. All authors

1232 contributed equally to the discussion and interpretation of data; M.Boss. provided Figs 6-11 and

1233 13; O.L. provided Figs 1, 2, information about stratigraphy and locality, MacClade analysis for

1234 ancestor-descendant relationships, and helped in the realization of Figs 6-11, and provided

1235 photographs then used in Figs 3-5; M.Bis. provided Figs 3-5, 12, 14, phylogenetic analysis,

1236 description, comparisons and wrote the paper.

1237

1238 **References**

1239

1240 Abel O. 1941. Vorläufige Mitteilungen über die Revision der fossilen Mystacoceten aus dem

1241 Tertiär Belgiens. *Bulletin du Museum Royal d'Histoire Naturelles de Belgique* 24(17):1–29.

1242 Benke H. 1993. Investigations on the osteology and the functional morphology of the flipper of

1243 whales and dolphins (Cetacea). *Investigations on Cetacea* 24:9–252.

1244 Bisconti M. 2000. New description, character analysis and preliminary phyletic assessment of two

1245 Balaenidae skulls from the Italian Pliocene. *Palaeontographia Italica* 87:37–66.

1246 Bisconti M. 2002. An early late Pliocene right whale (Genus *Eubalaena*) from Tuscany (Central

1247 Italy). *Bollettino della Società Paleontologica Italiana* 4:83–91.

1248 Bisconti M. 2003. Evolutionary history of Balaenidae. *Cranium* 20:9–50.

1249 Bisconti M. 2005a. Morphology and phylogenetic relationships of a new diminutive balaenid from

1250 the lower Pliocene of Belgium. *Palaeontology* 48:793–816.

1251 Bisconti M. 2005b. Paleontologia e conservazione: il caso della balena della Groenlandia. Pp. 133–

1252 142 in Scapini F. (ed.), La logica dell'evoluzione dei viventi – Spunti di Riflessione. Atti del

1253   XII Convegno del Gruppo Italiano di Biologia Evoluzionistica. Firenze University Press,

1254   Firenze, 167 pp.

1255 Bisconti M. 2007. A new basal balaenopterid from the Early Pliocene of northern Italy.

1256   *Palaeontology* 50:1103–1122.

1257 Bisconti M. 2008. Morphology and phylogenetic relationships of a new eschrichtiid genus

1258   (Cetacea: Mysticeti) from the Early Pliocene of northern Italy. *Zoological Journal of the*

1259   *Linnean Society* 153:161–186.

1260 Bisconti M. 2011. New description of *'Megaptera' hubachi* Dathe, 1983 based on the holotype

1261   skeleton held in the Museum für Naturkunde, Berlin. In: Bisconti M, Roselli A, Borzatti de

1262   Loewenstern A, eds. *Climatic Change, Biodiversity, Evolution: Natural History Museum*

1263   *and Scientific Research. Proceedings of the Meeting. Quaderni del Museo di Storia Naturale*

1264   *di Livorno* 23:37–68.

1265 Bisconti M. 2012. Comparative osteology and phylogenetic relationships of *Miocaperea pulchra*,

1266   the first fossil pygmy right whale genus and species (Cetacea, Mysticeti, Neobalaenidae).

1267   *Zoological Journal of the Linnean Society* 166:876–911.

1268 Bisconti M. 2015. Anatomy of a new cetotheriid genus and species from the Miocene of Herentals,

1269   Belgium, and the phylogenetic and paleobiogeographic relationships of Cetotheriidae s.s.

1270   (Mammalia, Cetacea, Mysticeti). *Journal of Systematic Palaeontology* 13:377–395.

1271 Bisconti M, Bosselaers M. 2016. *Fragilicetus velponi*: a new mysticete genus and species and its

1272   implications for the origin of Balaenopteridae (Mammalia, Cetacea, Mysticeti). *Zoological*

1273   *Journal of the Linnean Society* 177:450–474.

1274 Bisconti M, Francou C. 2014. I cetacei fossili conservati presso il Museo Geologico di

1275   Castell'Arquato (PC). *Museologia Scientifica Memorie* 13:31–36.

1276 Bisconti M, Lambert O, Bosselaers M. 2013. Taxonomic revision of *Isocetus depawi* (Mammalia,

1277   Cetacea, Mysticeti) and the phylogenetic relationships of archaic 'cetothere' mysticetes.

1278   *Palaeontology* 56:95–127.

1279 Boessenecker R, Fordyce RE. 2016. A new eomysticetid from the Oligocene Kokoamu Greensand

1280   of New Zealand and a review of the Eomysticetidae (Mammalia, Cetacea). *Journal of*

1281   *Systematic Palaeontology*. DOI: http://dx.doi.org/10.1080/14772019.2016.1191045.

1282 Boessenecker RW, Fordyce RE. 2015. A new genus and species of eomysticetid (Cetacea:

1283   Mysticeti) and a reinterpretation of *'Mauicetus' lophocephalus* Marples, 1956: transitional

1284   baleen whales from the Upper Oligocene of New Zealand. *Zoological Journal of the Linnean*

1285   *Society*. DOI: 10.1111/zoj.12297.

1286 Brisson AD. 1762. *Regnum animale in classes IX Distributum, sive synopsis methodica*. Leiden:

1287   Theodorum Haak.

1288 Chicchi S, Bisconti M. 2014. Valentina, una balena fossile nelle collezioni dei Musei Civici di

1289   Reggio Emilia. *Museologia Scientifica Memorie* 13:54–55.

1290 Churchill M, Berta A, Deméré TD. 2012. The systematics of right whales (Mysticeti: Balaenidae).

1291   *Marine Mammal Science* 28:497–521.

1292 Cioppi E. 2014. I cetacei fossili a Firenze, una storia lunga più di 250 anni. *Museologia Scientifica*

1293   *Memorie* 13:81–89.

1294 Clapham PJ, Young SB, Brownell RL Jr. 1999. Baleen whales: conservation issues and the status

1295   of the most endangered populations. *Mammal Review* 29:35–60.

1296 Cope ED. 1891. *Syllabus of Lectures on Geology and Paleontology*. Philadelphia: Ferris Brothers.

1297 Cuvier G. 1823. *Recherches sur les ossemens fossils*. Paris: Chez Deterville.

1298   Deméré TA, Berta A, McGowen MR. 2005. The taxonomic and evolutionary history of fossil and

1299   modern balaenopteroid mysticetes. *Journal of Mammalian Evolution* 12:99–143.

1300   De Schepper S, Head MJ, Louwye S (2009). Pliocene dinoflagellate cyst stratigraphy,

1301   palaeoecology and sequence stratigraphy of the Tunnel-Canal Dock, Belgium. *Geological*

1302   *magazine* 146:92–112.

1303   Desmoulins A. 1822. Baleine. *Dictionnaire Classique d'Histoire Naturelle*. Paris: Baudouin

1304   Frères.

1305   El Adli JJ, Deméré TA, Boessenecker RW. 2014. *Herpetocetus morrowi* (Cetacea: Mysticeti), a

1306   new species of diminutive baleen whale from the Upper Pliocene (Piacenzian) of

1307   California, USA, with observations on the evolution and relationships of the Cetotheriidae.

1308   *Zoological Journal of the Linnean Society* 170:400–466.

1309   Evans AR, Jones D, Boyer AG, Brown JH, Costa DP, Morgan ESK, Fitzgerald EMG, Fortelius

1310   M, Gittleman JL, Hamilton MJ, Harding ME, Lintulaakso K, Kathleen Lyons S, Okie JG,

1311   Saarinen JJ, Sibly RM, Smith FA, Stephens PR, Theodor JM, Uhen MD. 2012. The

1312   maximum rate of mammal evolution. *PNAS* 109:4187–4190.

1313   Fitch WM. 1971. Toward defining the course of evolution: minimum change for a specific tree

1314   topology. *Systematic Zoology* 20:406–416.

1315   Flower WH. 1864. Notes on the skeletons of whales in the principal museums of Holland and

1316   Belgium, with descriptions of two species apparently new to science. *Proceedings of the*

1317   *Zoological Society of London* 1864:384–420.

1318   Fordyce RE, & de Muizon C. 2001. Evolutionary history of cetaceans: a review. Pp. 169–234 in

1319   J.-M. Mazin and V. de Buffrenil (eds.). Secondary adaptation of tetrapods to life in water.

1320   Verlag Dr. Friedrich Pfeil, Munich.

Fraser FC, Purves PE. 1960. Hearing in cetaceans. *Bulletin of the British Museum (Natural History), Zoology* 7:1–140.

Gaines CA, Hare MP, Beck SE, Rosenbaum HC (2005) Nuclear markers confirm taxonomic status and relationships among highly endangered and closely related right whale species. *Proceedings of the Royal Society of London. Series B, Biological Sciences* 272:533–542.

Gaskin DE. 1986. The ecology of whales and dolphins. London: Heineman.

Geisler, J. & Sanders, A. E. 2003. Morphological evidence for the phylogeny of Cetacea. *Journal of Mammalian Evolution* 10:23–129.

Gol'din P, Startsev D, Krakhmalnaya T. 2014. The anatomy of the Late Miocene baleen whale *Cetotherium riabinini* from Ukraine. *Acta Palaeontologica Polonica* 59:795–814.

Gol'din P, Steeman ME. 2015. From problem taxa to problem solver: a new Miocene family, Tranatocetidae, brings perspective on baleen whale evolution. *PLOS ONE* 10(9):e0135500. DOI:10.1371/journal.pone.0135500.

Goloboff PA, Farris JS, Nixon KC. 2008. TNT, a free program for phylogenetic analysis. *Cladistics* 24:774–786.

Gray JE. 1864. On the Cetacea which have been observed in the seas surrounding the British Islands. *Proceedings of the Scientific Meetings of the Zoological Society of London* 1864:195–248

Gray JE. 1825. Outline of an attempt at the disposition of the Mammalia into tribes and families with a list of the genera apparently appertaining to each tribe. *Philosophical Annals* 26:337–344.

1342 Haile-Selassie Y, Melillo SM, Su DF. 2016. The Pliocene hominin diversity conundrum: do more

1343   fossils mean less clarity. *Proceedings of the National Academy of Sciences USA* 113:6364–

1344   6371.

1345 Hall BK. (ed.) 1996. Homology. Wiley, New York, 266 pp.

1346 Hasse G. 1909. Les morses du Pliocène poederlien à Anvers. *Bulletin de la Société Belge de*

1347   *Géologie, de Paléontologie et d'Hydrogéologie* 23:293–322.

1348 Heath T, Shannon A, Hedtke M, Hillis DM. 2008. Taxon sampling and the accuracy of

1349   phylogenetic analyses. *Journal of Systematics and Evolution* 46:239–257.

1350 Heinzelin J de. 1950. Stratigraphie pliocene et quaternaire observée au Kruisschans. I. Analyse

1351   stratigraphique; II. Conclusions. *Bulletin de l'Institut Royal des Sciences Naturelles de*

1352   *Belgique,* 26(40-41):1–60.

1353 Heinzelin J de. 1952. Note sur les coupes de l'écluse Baudouin à Anvers. *Bulletin de la Société*

1354   *Belge de Géologie* 61(1):106–108.

1355 Heinzelin J de. 1955a. Considérations nouvelles sur le Néogène de l'Ouest de l'Europe. *Bulletin de*

1356   *la Société Belge de Géologie* 64:463–476.

1357 Heinzelin J de. 1955b. Deuxième série d'observations stratigraphiques au Kruisschans. Coupes de

1358   l'écluse Baudouin. I. Analyse stratigraphique; II. Conclusions. *Bulletin de l'Institut Royal des*

1359   *Sciences Naturelles de Belgique* 31(66-67):1–43.

1360 Huelsenbeck JP. 1994. Comparing the stratigraphic record to estimates of phylogeny.

1361   *Paleobiology* 20:470–483.

1362 Jackson JA, Baker CS, Vant M, Steel DJ, Medrano-Gonzalez L, Palumbi SR. 2009. Big and slow:

1363   Estimates of molecular evolution in baleen whales (suborder Mysticeti). *Molecular Biology*

1364   *and Evolution* 26:2427–2440.

1365 Kaliszewska ZA, Seger J, Rowntree VJ, Barco SG, Benegas R, Best PB, Brown MW, Brownell
1366   RL Jr, Carribero A, Harcourt R, Knowlton AR, Marshalltilas K, Patenaude NJ, Rivarola M,
1367   Schaeff CM, Sironi M, Smith WA, Yamada TK. 2005. Population histories of right whales
1368   (Cetacea: *Eubalaena*) inferred from mitochondrial sequence diversities and divergences of
1369   their whale lice (Amphipoda: *Cyamus*). *Molecular Ecology* 14:3439–3456.

1370 Keane M, Semeiks J, Webb AE, Li YI, Quesada V, Craig T, Madsen LB, van Dam S, Brawand D,
1371   Marques PI, Michalak P, Kang L, Bhak J, Yim H-S, Grishin NV, Nielsen NH, Heide-
1372   Jørgensen MP, Oziolor EM, Matson CW, Church GM, Stuart GW, Patton JC, George JC,
1373   Suydam R, Larsen K, Lòpez-Otìn C, O'Connell MJ, Bickham JW, Thomsen B, de Magalhães
1374   JP. 2015. Insights into the Evolution of Longevity from the Bowhead Whale Genome. *Cell*
1375   *Reports* 10:112–122.

1376 Kellogg R. 1928. The history of whales – their adaptation to life in the water. *Quarterly Review of*
1377   *Biology* 3:29–76; and 174–208.

1378 Kenney RD. 2009. North Atlantic, North Pacific, and Southern right whales. In: Perrin WF,
1379   Wursig B, Thewissen JGM, eds. *Encyclopedia of Marine Mammals*. San Diego: Academic
1380   Press, 806–813.

1381 Kimura T. 2009. Review of fossil balaenids from Japan with a re-description of *Eubalaena*
1382   *shinshuensis* (Mammalia, Cetacea, Mysticeti). *Quaderni del Museo di Storia Naturale di*
1383   *Livorno* 22:3–21.

1384 Laga P, Louwye S, Mostaert F. 2006. Disused Neogene and Quaternary regional stages from
1385   Belgium: Bolderian, Houthalenian, Antwerpian, Diestian, Deurnian, Kasterlian,
1386   Kattendijkian, Scaldisian, Poederlian, Merksemian and Flandrian. *Geologica Belgica,* 9:215–
1387   224.

1388 Lambert O. 2008. A new porpoise (Cetacea, Odontoceti, Phocoenidae) from the Pliocene of the

1389   North Sea. *Journal of Vertebrate Paleontology* 28:863–872.

1390 Linnaeus C. 1758. *Systema Naturae*. Stockholm: Salvii.

1391 Maddison DR, Maddison WP. 2000. *MacClade 4: Analysis of phylogeny and character evolution.*

1392   *Version 4.0*. Sunderland: Sinauer Associates.

1393 Malik, S., Brown, M.W., Kraus, S.D. & B.N. White, 2000. Analysis of mitochondrial DNA

1394   diversity within and between North and South Atlantic right whales. *Marine Mammal Science*

1395   16:545–559.

1396 Manganelli G, Benocci A. 2014. I cetacei fossili del Museo dell'Accademia dei Fisiocritici di

1397   Siena. *Museologia Scientifica Memorie* 13:103–110.

1398 Marx FG. 2011. The more the merrier? A large cladistics analysis of mysticetes, and comments on

1399   the transition from teeth to baleen. *Journal of Mammalian Evolution* 18:77–100.

1400 Marx FG, Fordyce RE 2015. Baleen boom and bust: a synthesis of mysticete phylogeny, diversity

1401   and disparity. *Royal Society Open Science* 2:140434.

1402 Marx FG, Fordyce RE. 2016. A link no longer missing: new evidence for the cetotheriid affinities

1403   of *Caperea*. *PLOS ONE* 11(10):e0164059. DOI:10.1371/journal.pone.0164059.

1404

1405 McLeod SA, Whitmore FC Jr, Barnes LG. 1993. Evolutionary relationships and classification. In:

1406   Burns JJ, Montague JJ, Cowles CJ eds. *The Bowhead whale*. *The Society for Marine*

1407   *Mammalogy, Special Publication* 2:45–70.

1408 Mead JG, Fordyce RE. 2010. The therian skull. A lexicon with emphasis on the odontocetes.

1409   *Smithsonian Contributions to Zoology* 627:1–248.

1410 Miller GS. 1923. The telescoping of the cetacean skull. *Smithsonian Miscellaneous Collections*

1411   76:1–70.

1412 Misonne X. (1958). Faune du Tertiaire et du Pléistocène inférieur de Belgique (Oiseaux et

1413   Mammifères). *Bulletin de l'Institut Royal des Sciences Naturelles de Belgique* 34(5):1–36.

1414 Mitchell ED. 1989. A new cetacean from the late Eocene La Meseta Formation, Seymour Island,

1415   Antarctic Peninsula. *Canadian Journal of Fisheries and Aquatic Sciences* 46:2219–2235.

1416 Nishiwaki M, Hasegawa Y. 1969. The discovery of the right whale skull in the Kisagata shell bed.

1417   *The Scientific Reports of the Whale Research Institute Tokyo* 21:79–84.

1418 Omura H. 1958. North Pacific right whale. *The Scientific Reports of the Whale Research Institute*

1419   *Tokyo* 13:1– 52.

1420 Paul CRC. 1992. The recognition of ancestors. *Historical Biology* 6:239–250.

1421 Pivorunas A. 1979. The fibrocartilage skeleton and related structures of the ventral pouch of

1422   balaenopterid whales. *Journal of Morphology* 151:299–314.

1423 Plisnier-Ladame F, Quinet GE. 1969. *Balaena belgica* Abel 1938 Cetace du Merxemien d'Anvers.

1424   *Bulletin de l'Institut Royal des Sciences Naturelles de Belgique* 45(3):1–6.

1425 Pyenson ND, Sponberg SN. 2011. Reconstructing body size in extinct crown Cetacea (Neoceti)

1426   using allometry, phylogenetic methods, and tests from the fossil record. *Journal of*

1427   *Mammalian Evolution* 18:269–289.

1428 Quental TA, Marshall CR. 2010. Diversity dynamics: molecular phylogenies need the fossil

1429   record. *Trends in Ecology and Evolution* 25:434–441.

1430 Rice DW. 2009. Classification. In Perrin WF, Wursig B, Thewissen JGM eds. *Encyclopedia of*

1431   *Marine Mammals*. San Diego: Academic Press, 231–234.

1432   Rooney AP, Honeycutt RL, Derr JN. 2001. Population size change of Bowhead whales inferred

1433   from DNA sequence polymorphism data. *Evolution* 55:1678–1685.

1434   Rosenbaum HC, Brownell RL Jr, Brown MW, Schaeff C, Portway V, White BN, Malik S, Pastene

1435   LA, Patenaude NJ, Baker CS, Goto M, Best PB, Clapham PJ, Hamilton P, Moore M, Payne

1436   R, Rowntree V, Tynan CT, Bannister JL, Salle RD. 2000. World-wide genetic differentiation

1437   of *Eubalaena*: questioning the number of right whale species. *Molecular Ecology* 9:1793–

1438   1802.

1439   Sanderson LR, Wassersug R. 1993. Convergent and alternative designs for vertebrate suspension

1440   feeding. In: Hanken J, Hall BK eds. *The skull*. Vol. 3. Chicago: University Press of Chicago,

1441   37–112.

1442   Santangelo G, Bisconti M, Santini F, Bramanti L 2005. Estinzioni e conservazione: il ruolo dei

1443   modelli nello studio e nella tutela della diversità biologica. *Biology Forum* 98:13–18.

1444   Sarti C, Lanzetti A. 2014. I cetacei fossili del Museo Geologico Giovanni Capellini dell'Università

1445   di Bologna. *Museologia Scientifica Memorie* 13:70–78.

1446   Sasaki T, Nikaido M, Hamilton H, Goto M, Kato H, Kanda N, Pastene LA, Cao Y, Fordyce RE,

1447   Hasegawa M, Okada N. 2005. Mitochondrial phylogenetics and evolution of mysticete

1448   whales. *Systematic Biology* 54:77–90.

1449   Seehausen O. 2006. African cichlid fish: a model system in adaptive radiation research.

1450   *Proceedings of the Royal Society B* 273: DOI: 10.1098/rspb.2006.3539.

1451   Shaller O. 1999. *Nomenclatura anatomica veterinaria illustrate*. Roma: Antonio Delfino Editore.

1452   Silva M, Downing JA. 1995. The allometric scaling of density and body mass: a nonlinear

1453   relationship for terrestrial mammals. *The American Naturalist* 145:704–727.

1454 Steeman ME, Hebsgaard MB, Fordyce RE, Ho SYW, Rabosky DL, Nielsen R, Rahbek C, Glenner

1455   H, Sørensen MV, Willerslev E. 2009. Radiation of extant cetaceans driven by restructuring of

1456   the oceans. *Systematic Biology* 58:573–585.

1457 Tomilin AG. 1967. Cetacea. In: Heptner VG ed. *Mammals of the USSR and adjacent countries*.

1458   Vol. 9. Jerusalem: Israel Program for Scientific Translations, 1–717.

1459 True FW. 1904. The whalebone whales of the western north Atlantic, compared with those

1460   occurring in European waters; with some observations on the species of the north Pacific.

1461   *Smithsonian Contributions to Knowledge* 33:1–332.

1462 Tsai C-H, Fordyce RE. 2015. Ancestor-descendant relationships in evolution: origin of the extant

1463   pygmy right whale, *Caperea marginata*. *Biology Letters* 11:20140875. DOI:

1464   http://dx.doi.org/10.1098/rsbl.2014.0875.

1465 Uhen MD, Gingerich PD. 2001. New genus of dorudontine archaeocete (Cetacea) from the

1466   middle-to-late Eocene of South Carolina. *Marine Mammal Science* 17:1–34.

1467 Vandenberghe N, Laga P, Steurbaut E, Hardenbol J, Vail PR. 1998. Tertiary sequence stratigraphy

1468   at the southern border of the North Sea Basin in Belgium. *Special Publication-SEPM,* 60:119–

1469   154.

1470 Wagner PJ. 2000. Exhaustion of morphologic character states among fossil taxa. *Evolution*

1471   54:365–386.

1472 Zachos J, Pagani M, Sloan L, Thomas E, Billups K. 2001. Trends, rhythms, and aberrations in

1473   global climate 65 Ma to present. *Science* 292:686–693.

1474

1475

1476

1477

1478

1479 **CAPTIONS TO TEXT-FIGURES AND TABLES**

1480

1481 **Figure 1**

1482 Localities of the balaenids described in this paper. A, Localization of Antwerp in Belgium and its

1483 relationships with the North Sea. Grey whading represents marine Pliocene deposits. B, Detailed

1484 map of the Antwerp harbor showing the first Kruisschans lock, where the holotype of *Eubalaena*

1485 *ianitrix* sp. nov. (RBINS M. 879a-f) and the fragment of maxilla RBINS M. 880 were found. The

1486 cervical vertebrae RBINS M. 881 were discovered in the "Darses I-II" in Oorderen. Modified from

1487 De Schepper et al., 2009.

1488

1489 **Figure 2**

1490 Lithological units from the Pliocene of the Antwerp area. Formations, members and their ages are

1491 provided, including the Kruisschans Sands Member of the Lillo Formation in the Piacenzian (Late

1492 Pliocene), where the holotype of *Eubalaena ianitrix* sp. nov. was discovered. Modified from De

1493 Schepper et al., 2009.

1494

1495 **Figure 3**

1496 The cervical vertebrae RBINS M. 881 that were originally used as type of *'Balaena' belgica* by

1497 Abel (1941) and reassigned to Balaenidae gen. et sp. indet. in this work. A, anterior view. B, left

1498 lateral view. C, posterior view. D, right lateral view. E, ventral view. F, dorsal view. Scale bar

1499 equals 10 cm.

1500

1501 **Figure 4**

1502 The fragment of right maxilla RBINS M. 880 assigned to Balaenidae gen. et sp. indet. in this work.

1503 A, dorsolateral view. B, dorsomedial view. C, ventromedial view. Scale bar equals 30 cm.

1504

1505

1506 **Figure 5**

1507 The left humerus RBINS M. 2280 assigned to *Eubalaena* sp. in this work. A, lateral view. B,

1508 anterior view. C, distal view of articular facets for radius and ulna. D, proximal view or articular

1509 head for scapula. E, posterior view. F, medial view. Scale bars equal 10 cm.

1510

1511 **Figure 6**

1512 *Eubalaena ianitrix* sp. nov. (holotype RBINS M. 879). Dorsal view of neurocranium. A,

1513 photographic representation. B, interpretation. Scale bar equals 50 cm. Anatomical abbreviations:

1514 fm, foramen magnum; fr, frontal; irfr, interorbital region of the frontal; oc, occipital condyles; smc,

1515 supramastoid crest; sq, squamosal; sop, supraorbital process of the frontal.

1516

1517 **Figure 7**

1518 *Eubalaena ianitrix* sp. nov. (holotype RBINS M. 879). Left lateral view of neurocranium. A,

1519 photographic representation. B, interpretation. Scale bar equals 50 cm. Anatomical abbreviations:

1520 fm, foramen magnum; fr, frontal; irfr, interorbital region of the frontal; oc, occipital condyle; orb,

1521 orbit; otc, orbitotemporal crest; par, parietal; pgl, postglenoid process of squamosal; p-fr, parietal-

1522 frontal suture; p-sq, parietal-squamosal suture; smc, supramastoid crest; soc, supraoccipital; sop,

1523 supraorbital process of frontal; sq, squamosal; vom, vomer; zyg, zygomatic process of squamosal;

1524 *, anterolateral corner of parietal-frontal suture.

1525

1526 **Figure 8**

1527 *Eubalaena ianitrix* sp. nov. (holotype RBINS M. 879). Right lateral view of neurocranium. A,

1528 photographic representation. B, interpretation. Scale bar equals 50 cm. Anatomical abbreviations:

1529 fm, foramen magnum; fr, frontal; irfr, interorbital region of the frontal; oc, occipital condyle; orb,

1530 orbit; otc, orbitotemporal crest; par, parietal; pgl, postglenoid process of squamosal; p-fr, parietal-

1531 frontal suture; p-sq, parietal-squamosal suture; smc, supramastoid crest; soc, supraoccipital; sop,

1532 supraorbital process of frontal; sq, squamosal; vom, vomer; zyg, zygomatic process of squamosal;

1533 *, anterolateral corner of parietal-frontal suture.

1534

1535 **Figure 9**

1536 *Eubalaena ianitrix* sp. nov. (holotype RBINS M. 879). Anterior view of neurocranium. A,

1537 photographic representation. B, interpretation. Scale bar equals 50 cm. Anatomical abbreviations:

1538 fr, frontal; irfr, interorbital region of the frontal; max-fr, grooves for articulation of maxilla and

1539 frontal; mes, mesethmoid; nas-fr, groove for articulation of nasal and frontal; pal, palatine; par,

1540 parietal; pgl, postglenoid process of squamosal; pm-fr, grooves for articulation of premaxilla and

1541 frontal; soc, supraoccipital; sop, supraorbital process of frontal; sq, squamosal; vom, vomer; zyg,

1542 zygomatic process of squamosal.

1543

1544 **Figure 10.**

1545 *Eubalaena ianitrix* sp. nov. (holotype RBINS M. 879). Ventral view of neurocranium. A,

1546 photographic representation. B, interpretation. Scale bar equals 50 cm. Anatomical abbreviations:

1547 exo, exoccipital; fm, foramen magnum; fr, frontal; sop, supraorbital process of frontal; oc, occipital

1548   condyle; och, optic channel; or, orbit; pgl, postglenoid process of squamosal; pt, pterygoid; sq,

1549   squamosal; vom, vomer; zyg, zygomatic process of squamosal.

1550

1551   **Figure 11**

1552   *Eubalaena ianitrix* sp. nov. (holotype RBINS M. 879). Posterior view of neurocranium. A,

1553   photographic representation. B, interpretation. Scale bar equals 50 cm. Anatomical abbreviations:

1554   boc, basioccipital; bop, basioccipital protuberance; exo, exoccipital; fm, foramen magnum; fr,

1555   frontal; jn, jugular notch; oc, occipital condyle; pal, palatine; pgl, postglenoid process of

1556   squamosal; pt, pterygoid; ptf, pterygoid fossa; sop, supraorbital process of frontal; sq, squamosal;

1557   vom, vomer; zyg, zygomatic process of squamosal.

1558

1559   **Figure 12**

1560   Phylogenetic relationships of Mysticeti with focus on Balaenoidea. Single most-parsimonious

1561   cladogram with the following tree statistics: Consistency Index (CI), 0.508; Retention Index (RI),

1562   0.805; Rescaled CI, 0.40894; Homoplasy Index (HI), 0.492; Stratigraphic Consistency Index

1563   (SCI), 0.825.

1564

1565   **Figure 13**

1566   Schematic representation of diagnostic characters observed in the holotype skull of *Eubalaena*

1567   *ianitrix* in left lateral view. Character in thin black (115: presence of a dome on the supraoccipital)

1568   refer to the monophyly of *Eubalaena*; characters in solid black (126: vertical orientation of the

1569   squamosal; 127: squared exoccipital in lateral view) refer to the monophyly of *Eubalaena* sp. from

1570   Tuscany and the other crownward *Eubalaena* species; characters in Italics (125: presence of a

1571   distinctive corner at the anterolateral border of the parietal; 133: spreading of the parietal on the

1572   posteromedial surface of the supraorbital process of the frontal; 134: parietal projecting anteriorly)

1573   refer to the monophyly of the extant species of *Eubalaena + E. ianitrix*.

1574

1575   **Figure 14**

1576   Phylogenetic relationships of Balaenidae plotted against a time scale in million years (Ma). Bold

1577   lines represent stratigraphic ages of taxa based on dated specimens; light lines represent inferred

1578   presence of taxa. Note that three time periods are highlighted: (1) separation of Balaenidae and

1579   Neobalaenidae inferred to have occurred *c.* 11 Ma (latest Serravallian-to-earliest Tortonian); (2)

1580   separation of the *Balaena + Balaenella* clade and the *Eubalaena + Balaenula* clade inferred to

1581   have occurred *c.* 7 Ma (latest Tortonian-to-earliest Messinian); and (3) origin of the extant

1582   *Eubalaena* species inferred to have occurred *c.* 2.5 Ma (latest Zanclean-to-earliest Piacenzian).

1583

1584

1585   **Table 1**

1586   Measurements (in mm) of RBINS M. 880 (cervical vertebrae complex, Balaenidae gen. et sp.

1587   indet.) and M. 2280 (left humerus, *Eubalaena* sp.). Characters are measured as preserved.

1588

1589   **Table 2**

1590   Measurements (in mm) of the neurocranium RBINS M. 879a-f (holotype of *Eubalaena ianitrix*

1591   sp. nov.). Characters are measured as preserved.

1592

Figure 1

Localities of the balaenids described in this paper.

Fig. 1 - Localities of the balaenids described in this paper. A, Localization of Antwerp in Belgium and its relationships with the North Sea. Grey whading represents marine Pliocene deposits. B, Detailed map of the Antwerp harbor showing the first Kruisschans lock, where the holotype of *Eubalaena ianitrix* sp. nov. (RBINS M. 879a-f) and the fragment of maxilla RBINS M. 880 were found. The cervical vertebrae RBINS M. 881 were discovered in the "Darses I-II" in Oorderen. Modified from De Schepper et al., 2009.
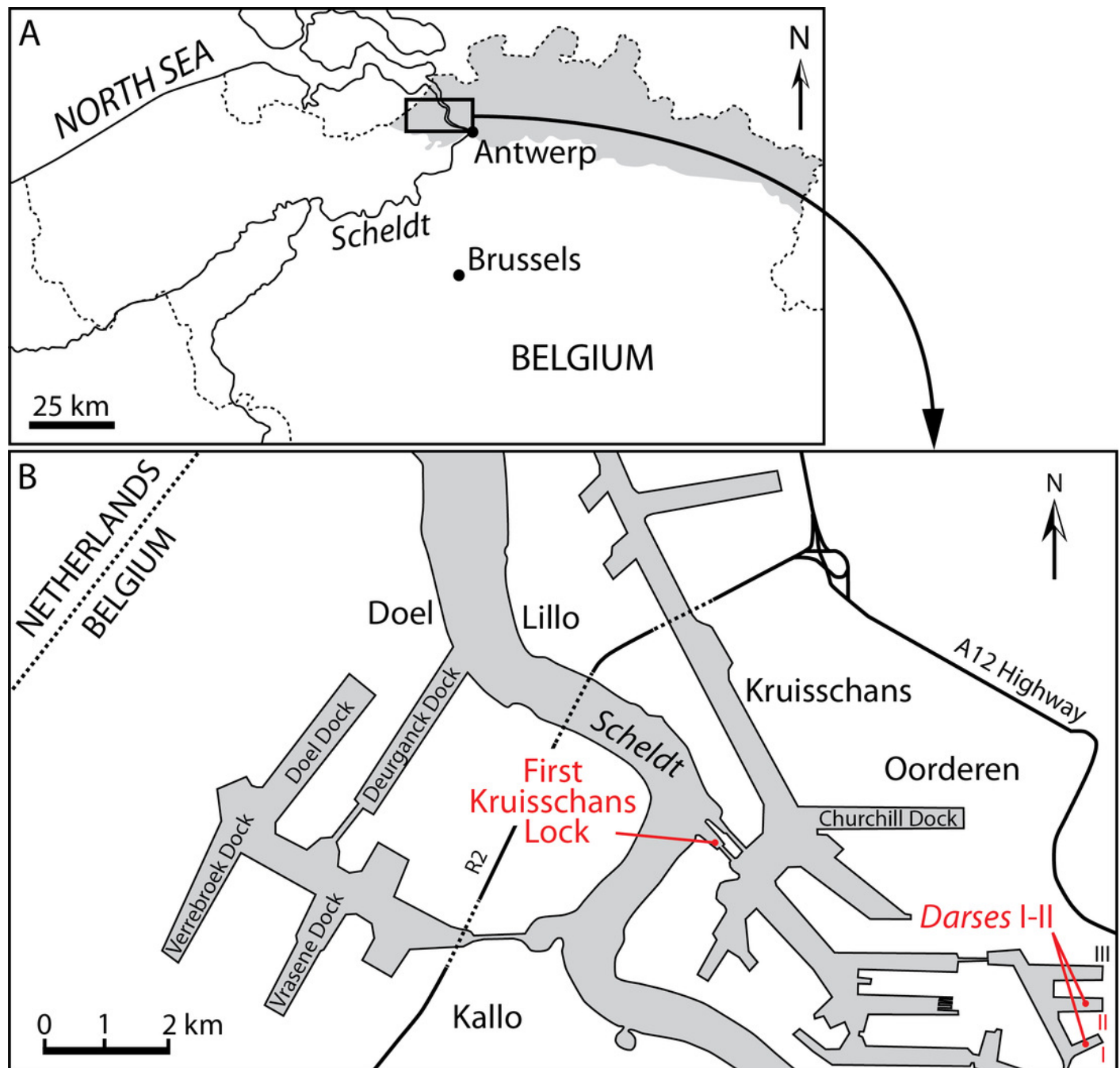
Figure 2

Lithological units from the Pliocene of the Antwerp area.

Fig. **2 -** Lithological units from the Pliocene of the Antwerp area. Formations, members and their ages are provided, including the Kruisschans Sands Member of the Lillo Formation in the Piacenzian (Late Pliocene), where the holotype of *Eubalaena ianitrix* sp. nov. was discovered. Modified from De Schepper et al., 2009.

Age (Ma)	EPOCH	AGE		FORMATION	MEMBERS
2.0 — 2.5 —	PLEIST.	EARLY	GELASIAN		
3.0 — 3.5 —	PLIOCENE	LATE	PIACENZIAN	Lillo Formation	Merksem Sands Member Kruisschans Sands Member Oorderen Sands Member Luchtbal Sands Member
4.0 — 4.5 — 5.0 —		EARLY	ZANCLEAN		
				Kattendijk Formation	
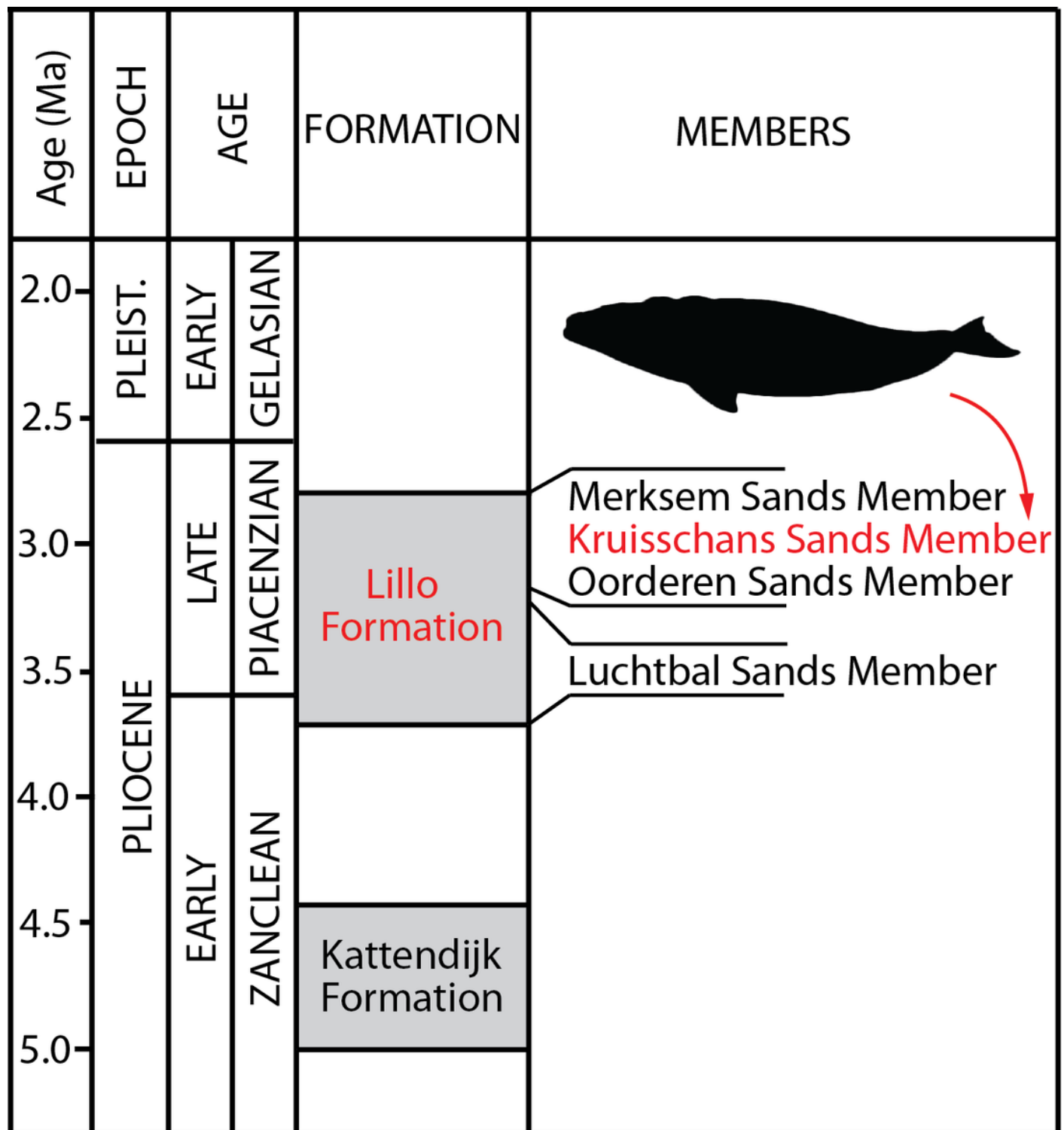
Figure 3

The cervical vertebrae RBINS M. 881.

Fig. 3 - The cervical vertebrae RBINS M. 881 that were originally used as type of *'Balaena'* *belgica* by Abel (1941) and reassigned to Balaenidae gen. et sp. indet. in this work. A, anterior view. B, left lateral view. C, posterior view. D, right lateral view. E, ventral view. F, dorsal view. Scale bar equals 10 cm.
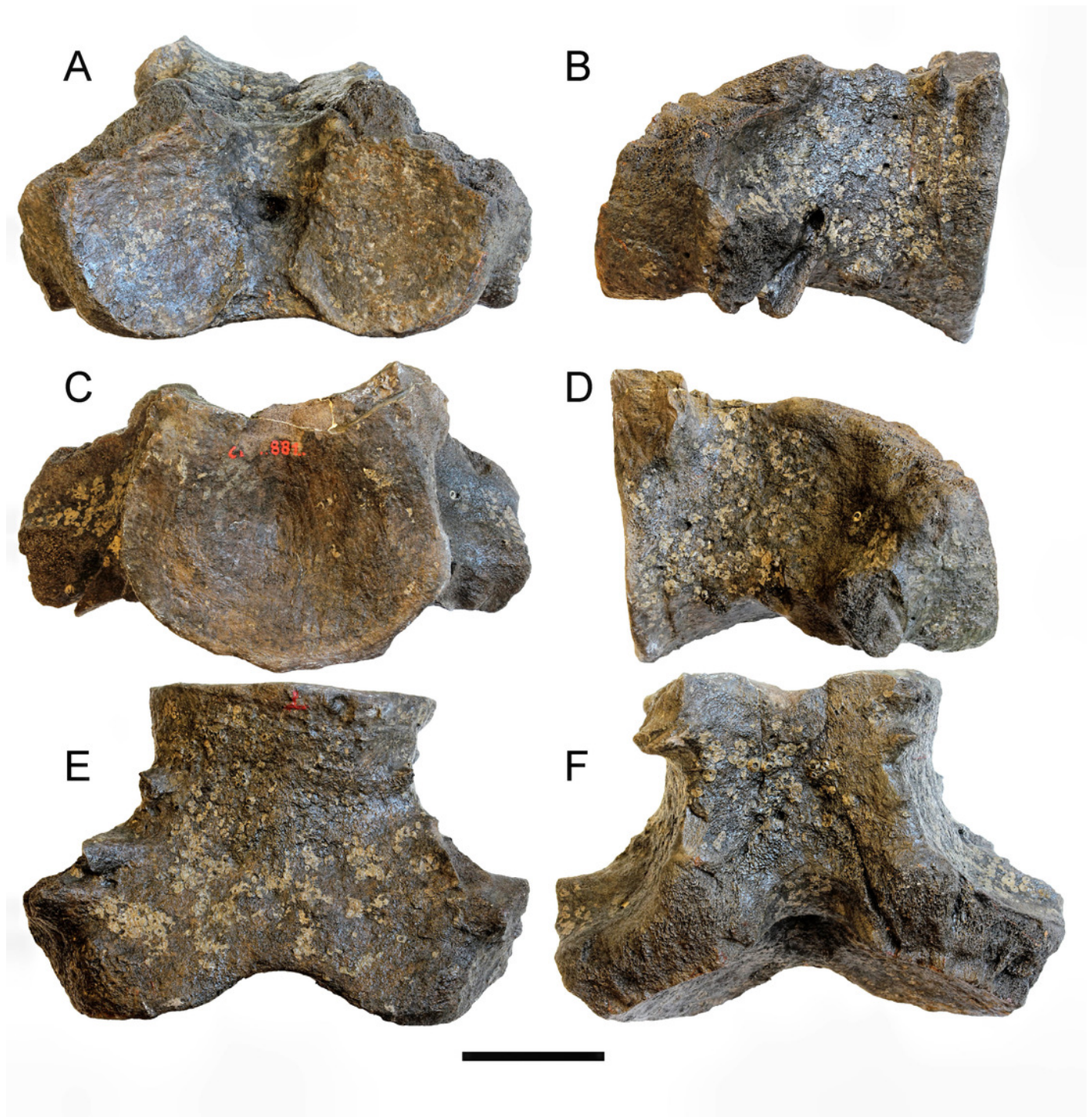
Figure 4

The fragment of right maxilla RBINS M. 880.

Fig. 4 - The fragment of right maxilla RBINS M. 880 assigned to Balaenidae gen. et sp. indet. in this work. A, dorsolateral view. B, dorsomedial view. C, ventromedial view. Scale bar equals 30 cm.

Figure 5

The left humerus RBINS M. 228.

Fig. 5 - The left humerus RBINS M. 2280 assigned to *Eubalaena* sp. in this work. A, lateral view. B, anterior view. C, distal view of articular facets for radius and ulna. D, proximal view or articular head for scapula. E, posterior view. F, medial view. Scale bars equal 10 cm.

Figure 6

Eubalaena ianitrix sp. nov. (holotype RBINS M. 879). Dorsal view of neurocranium.

Fig. 6 - *Eubalaena ianitrix* sp. nov. (holotype RBINS M. 879). Dorsal view of neurocranium. A, photographic representation. B, interpretation. Scale bar equals 50 cm. Anatomical abbreviations: fm, foramen magnum; fr, frontal; irfr, interorbital region of the frontal; oc, occipital condyles; smc, supramastoid crest; sq, squamosal; sop, supraorbital process of the frontal.
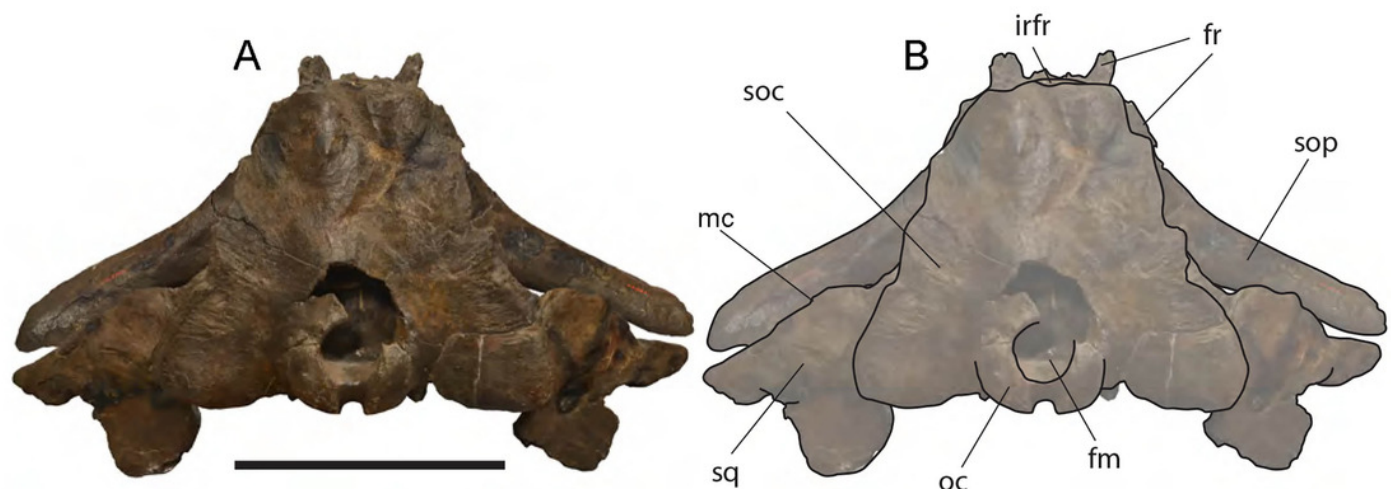
Figure 7

Eubalaena ianitrix sp. nov. (holotype RBINS M. 879). Left lateral view of neurocranium.

Fig. 7 - *Eubalaena ianitrix* sp. nov. (holotype RBINS M. 879). Left lateral view of neurocranium. A, photographic representation. B, interpretation. Scale bar equals 50 cm. Anatomical abbreviations: fm, foramen magnum; fr, frontal; irfr, interorbital region of the frontal; oc, occipital condyle; orb, orbit; otc, orbitotemporal crest; par, parietal; pgl, postglenoid process of squamosal; p-fr, parietal-frontal suture; p-sq, parietal-squamosal suture; smc, supramastoid crest; soc, supraoccipital; sop, supraorbital process of frontal; sq, squamosal; vom, vomer; zyg, zygomatic process of squamosal; *, anterolateral corner of parietal-frontal suture.
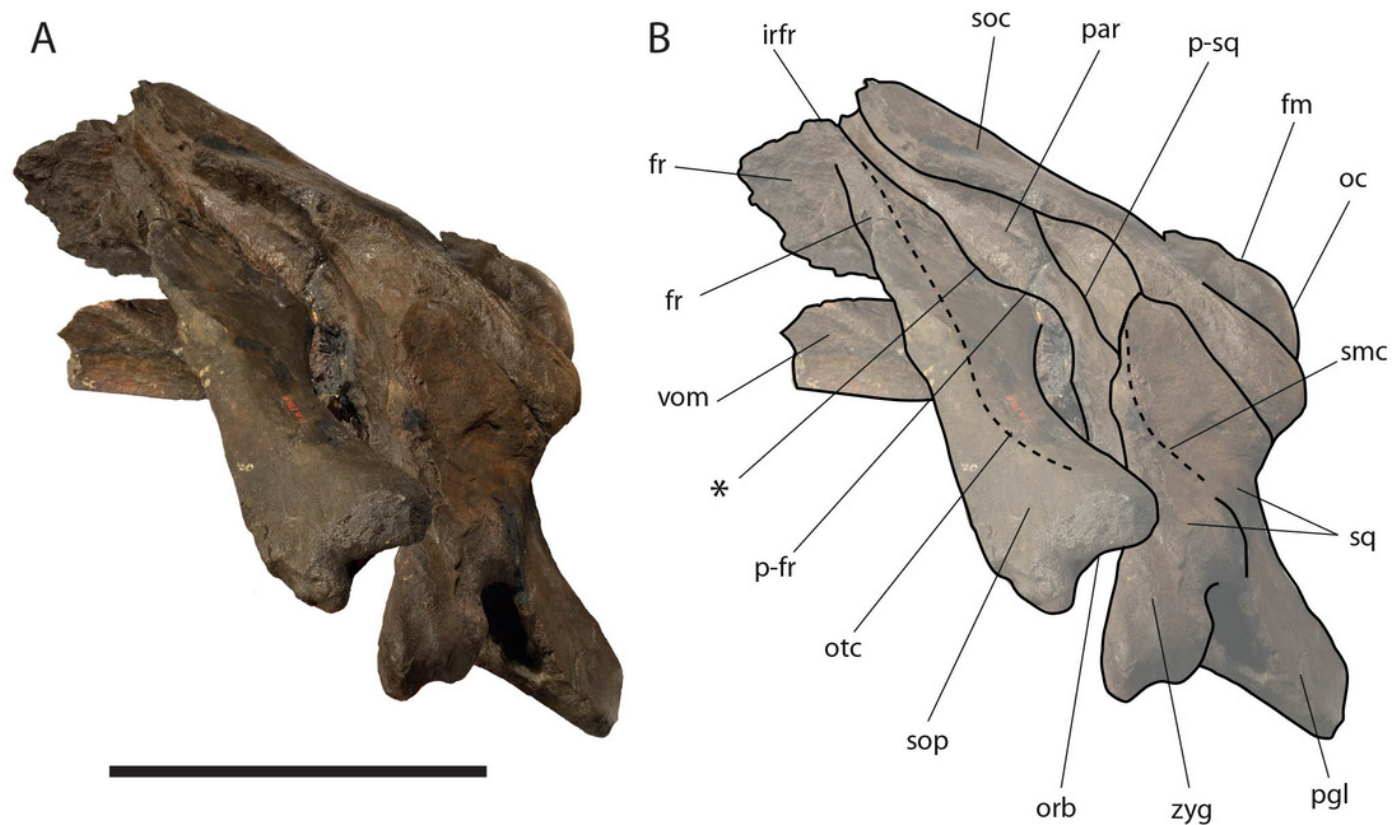
Figure 8

Eubalaena ianitrix sp. nov. (holotype RBINS M. 879). Right lateral view of neurocranium.

Fig. 8 - *Eubalaena ianitrix* sp. nov. (holotype RBINS M. 879). Right lateral view of neurocranium. A, photographic representation. B, interpretation. Scale bar equals 50 cm. Anatomical abbreviations: fm, foramen magnum; fr, frontal; irfr, interorbital region of the frontal; oc, occipital condyle; orb, orbit; otc, orbitotemporal crest; par, parietal; pgl, postglenoid process of squamosal; p-fr, parietal-frontal suture; p-sq, parietal-squamosal suture; smc, supramastoid crest; soc, supraoccipital; sop, supraorbital process of frontal; sq, squamosal; vom, vomer; zyg, zygomatic process of squamosal; *, anterolateral corner of parietal-frontal suture.
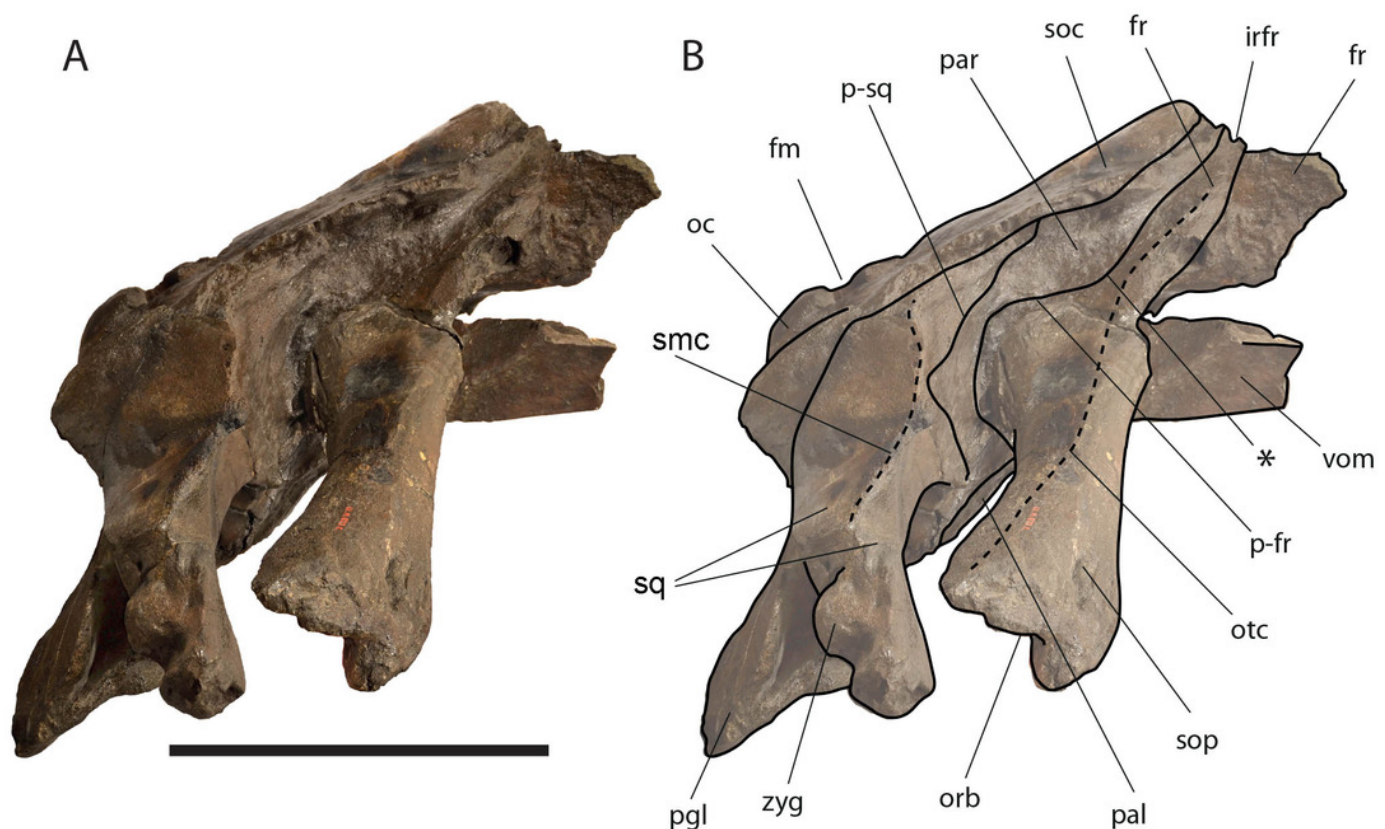
Figure 9

Eubalaena ianitrix sp. nov. (holotype RBINS M. 879). Anterior view of neurocranium.

Fig. 9 - *Eubalaena ianitrix* sp. nov. (holotype RBINS M. 879). Anterior view of neurocranium. A, photographic representation. B, interpretation. Scale bar equals 50 cm. Anatomical abbreviations: fr, frontal; irfr, interorbital region of the frontal; max-fr, grooves for articulation of maxilla and frontal; mes, mesethmoid; nas-fr, groove for articulation of nasal and frontal; pal, palatine; par, parietal; pgl, postglenoid process of squamosal; pm-fr, grooves for articulation of premaxilla and frontal; soc, supraoccipital; sop, supraorbital process of frontal; sq, squamosal; vom, vomer; zyg, zygomatic process of squamosal.
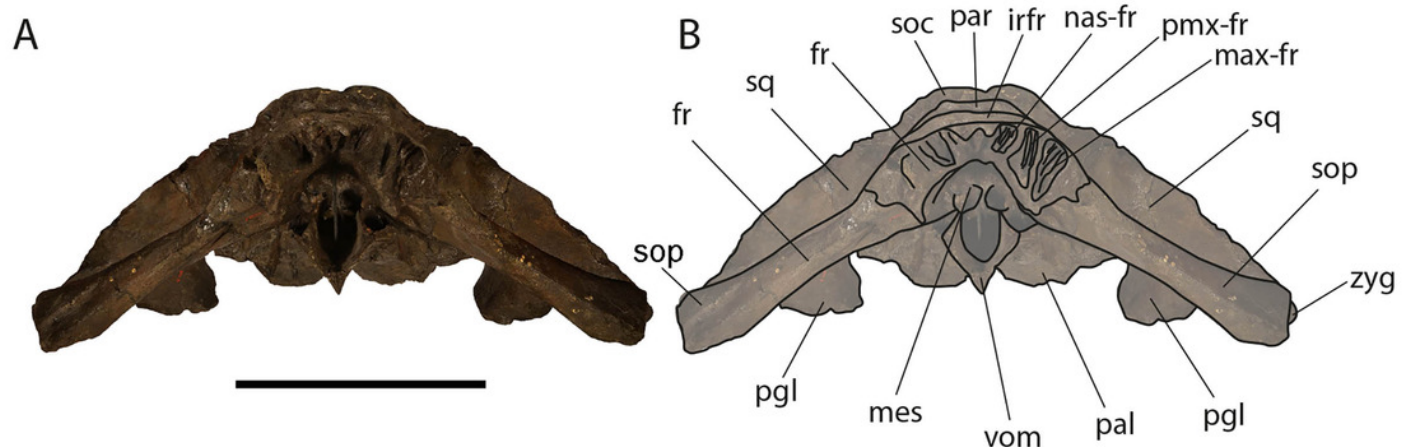
Figure 10

Eubalaena ianitrix sp. nov. (holotype RBINS M. 879). Ventral view of neurocranium.

Fig. 10 - *Eubalaena ianitrix* sp. nov. (holotype RBINS M. 879). Ventral view of neurocranium. A, photographic representation. B, interpretation. Scale bar equals 50 cm. Anatomical abbreviations: exo, exoccipital; fm, foramen magnum; fr, frontal; sop, supraorbital process of frontal; oc, occipital condyle; och, optic channel; or, orbit; pgl, postglenoid process of squamosal; pt, pterygoid; sq, squamosal; vom, vomer; zyg, zygomatic process of squamosal.
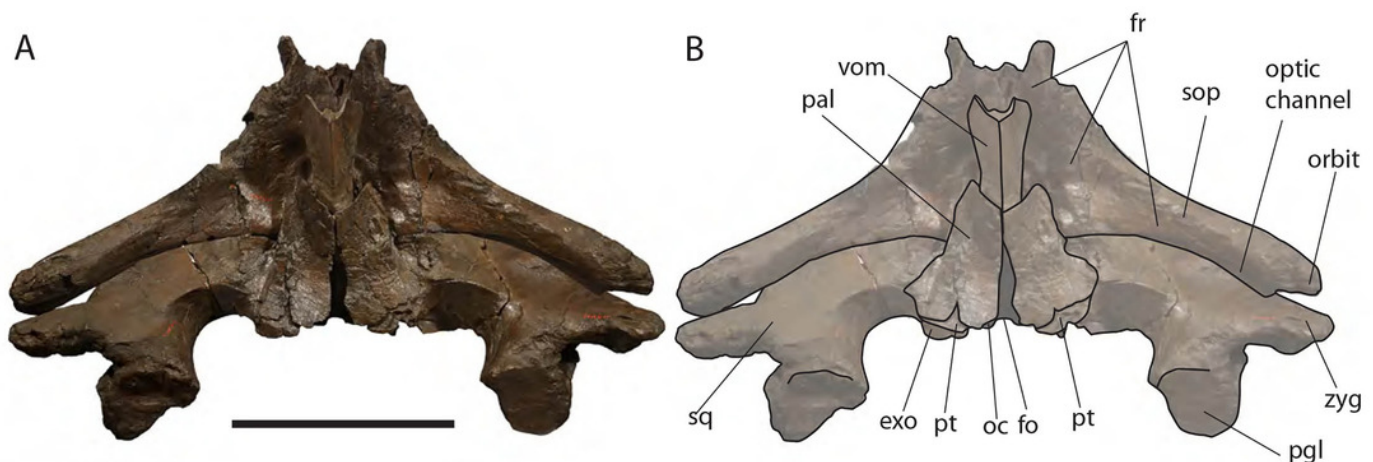
Figure 11

Eubalaena ianitrix sp. nov. (holotype RBINS M. 879). Posterior view of neurocranium.

Fig. 11 - *Eubalaena ianitrix* sp. nov. (holotype RBINS M. 879). Posterior view of neurocranium. A, photographic representation. B, interpretation. Scale bar equals 50 cm. Anatomical abbreviations: boc, basioccipital; bop, basioccipital protuberance; exo, exoccipital; fm, foramen magnum; fr, frontal; jn, jugular notch; oc, occipital condyle; pal, palatine; pgl, postglenoid process of squamosal; pt, pterygoid; ptf, pterygoid fossa; sop, supraorbital process of frontal; sq, squamosal; vom, vomer; zyg, zygomatic process of squamosal.
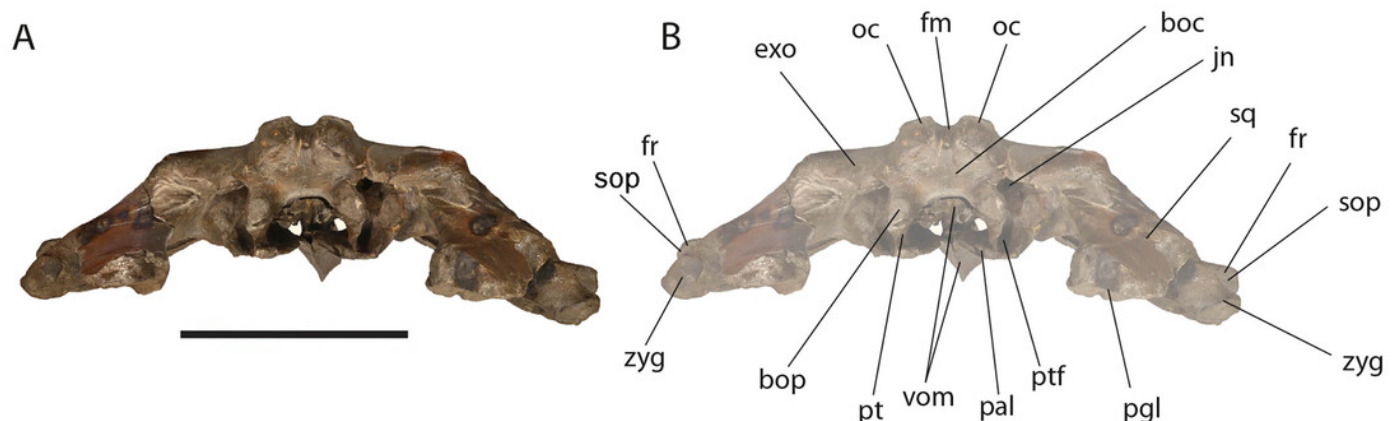
Figure 12

Phylogenetic relationships of Mysticeti with focus on Balaenoidea.

Fig. 12 - Phylogenetic relationships of Mysticeti with focus on Balaenoidea. Single most-parsimonious cladogram with the following tree statistics: Consistency Index (CI), 0.508; Retention Index (RI), 0.805; Rescaled CI, 0.40894; Homoplasy Index (HI), 0.492; Stratigraphic Consistency Index (SCI), 0.825.
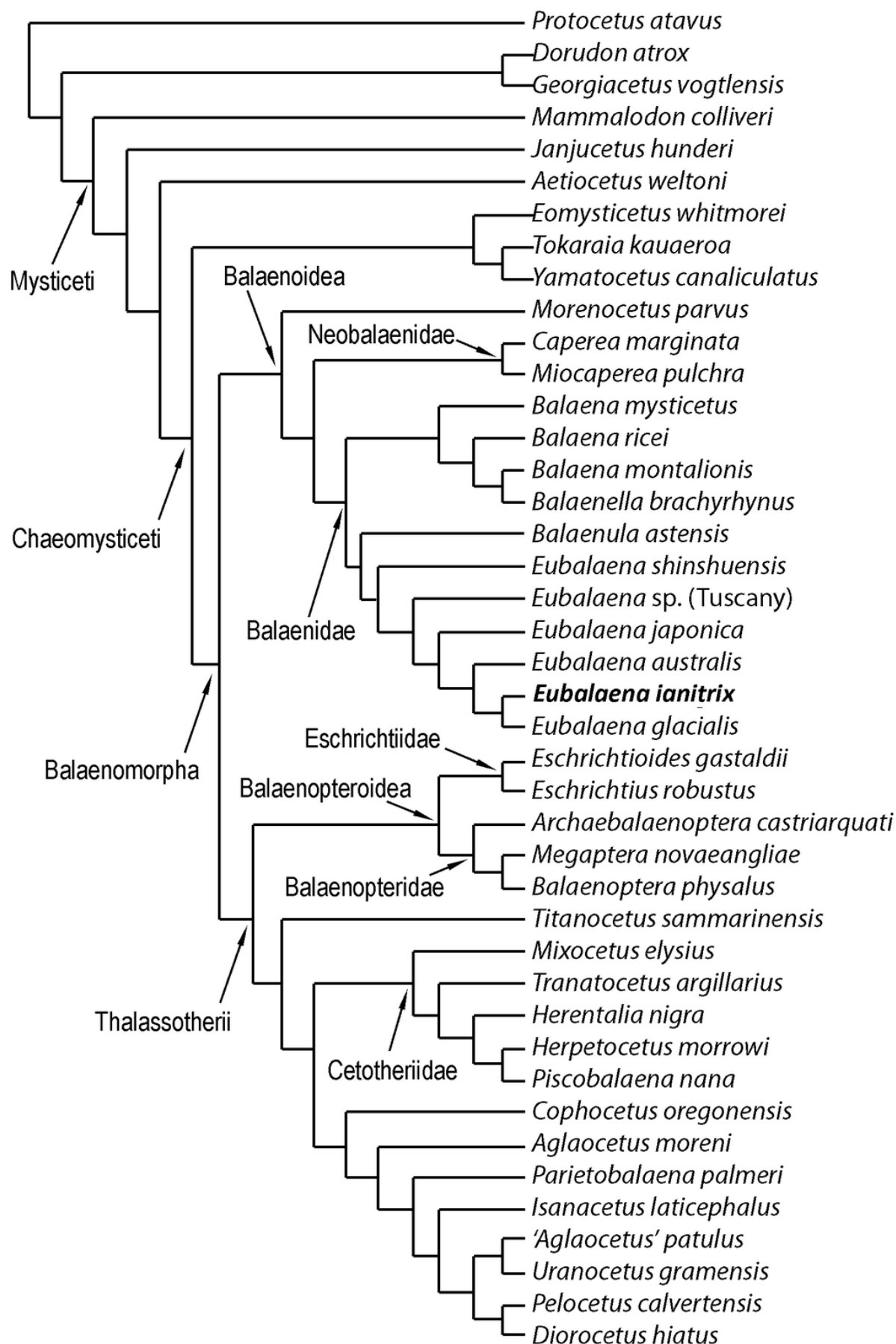
Figure 13

Schematic representation of diagnostic characters observed in the holotype skull of *Eubalaena ianitrix* in left lateral view.

Fig. 13 - Schematic representation of diagnostic characters observed in the holotype skull of *Eubalaena ianitrix* in left lateral view. Character in thin black (115: presence of a dome on the supraoccipital) refer to the monophyly of *Eubalaena*; characters in solid black (126: vertical orientation of the squamosal; 127: squared exoccipital in lateral view) refer to the monophyly of *Eubalaena* sp. from Tuscany and the other crownward *Eubalaena* species; characters in Italics (125: presence of a distinctive corner at the anterolateral border of the parietal; 133: spreading of the parietal on the posteromedial surface of the supraorbital process of the frontal; 134: parietal projecting anteriorly) refer to the monophyly of the extant species of *Eubalaena + E. ianitrix*.
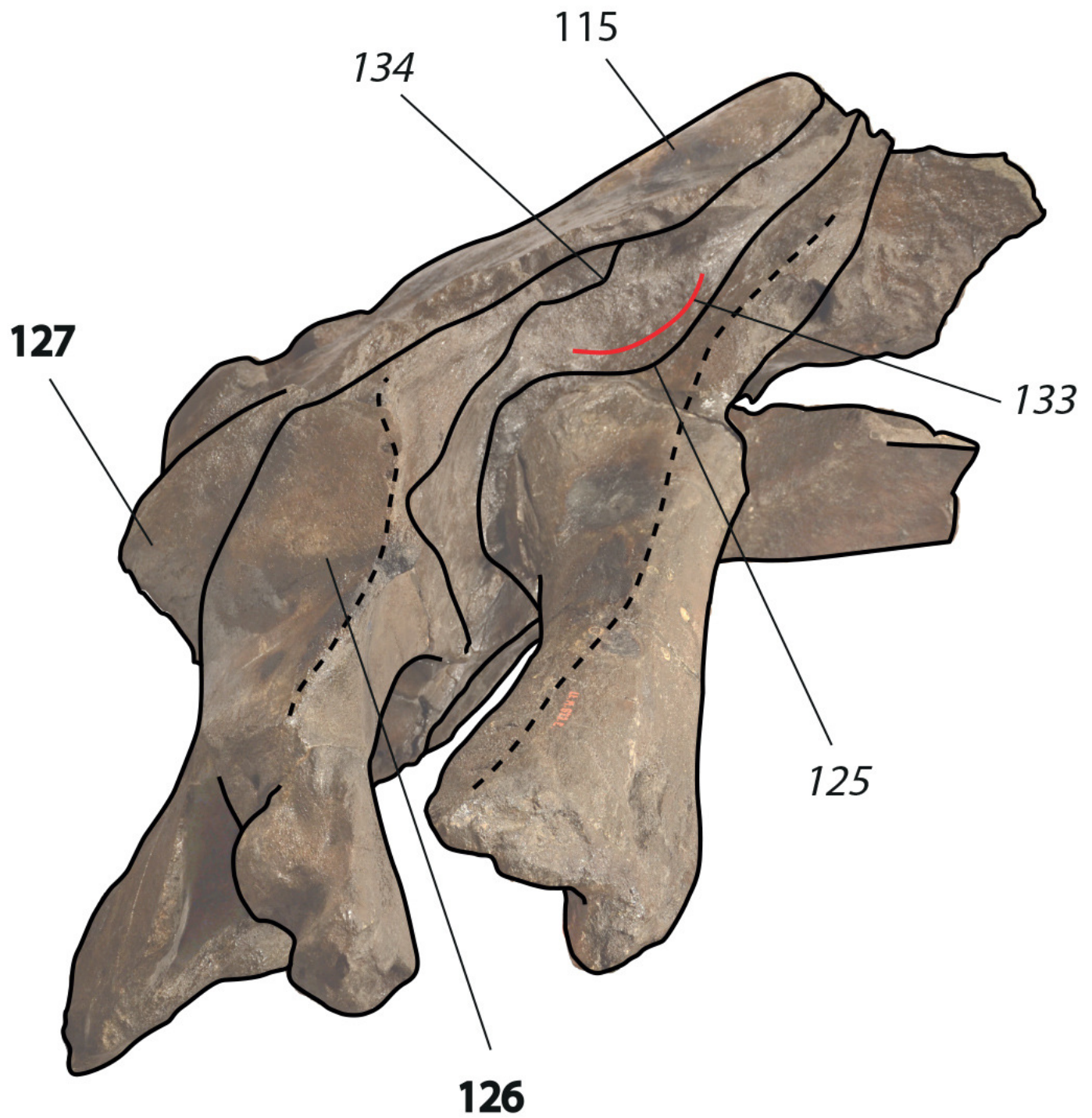
Figure 14

Phylogenetic relationships of Balaenidae plotted against a time scale in million years (Ma).

Fig. 14 - Phylogenetic relationships of Balaenidae plotted against a time scale in million years (Ma). Bold lines represent stratigraphic ages of taxa based on dated specimens; light lines represent inferred presence of taxa. Note that three time periods are highlighted: (1) separation of Balaenidae and Neobalaenidae inferred to have occurred *c.* 11 Ma (latest Serravallian-to-earliest Tortonian); (2) separation of the *Balaena + Balaenella* clade and the *Eubalaena + Balaenula* clade inferred to have occurred *c.* 7 Ma (latest Tortonian-to-earliest Messinian); and (3) origin of the extant *Eubalaena* species inferred to have occurred *c.* 2.5 Ma (latest Zanclean-to-earliest Piacenzian).
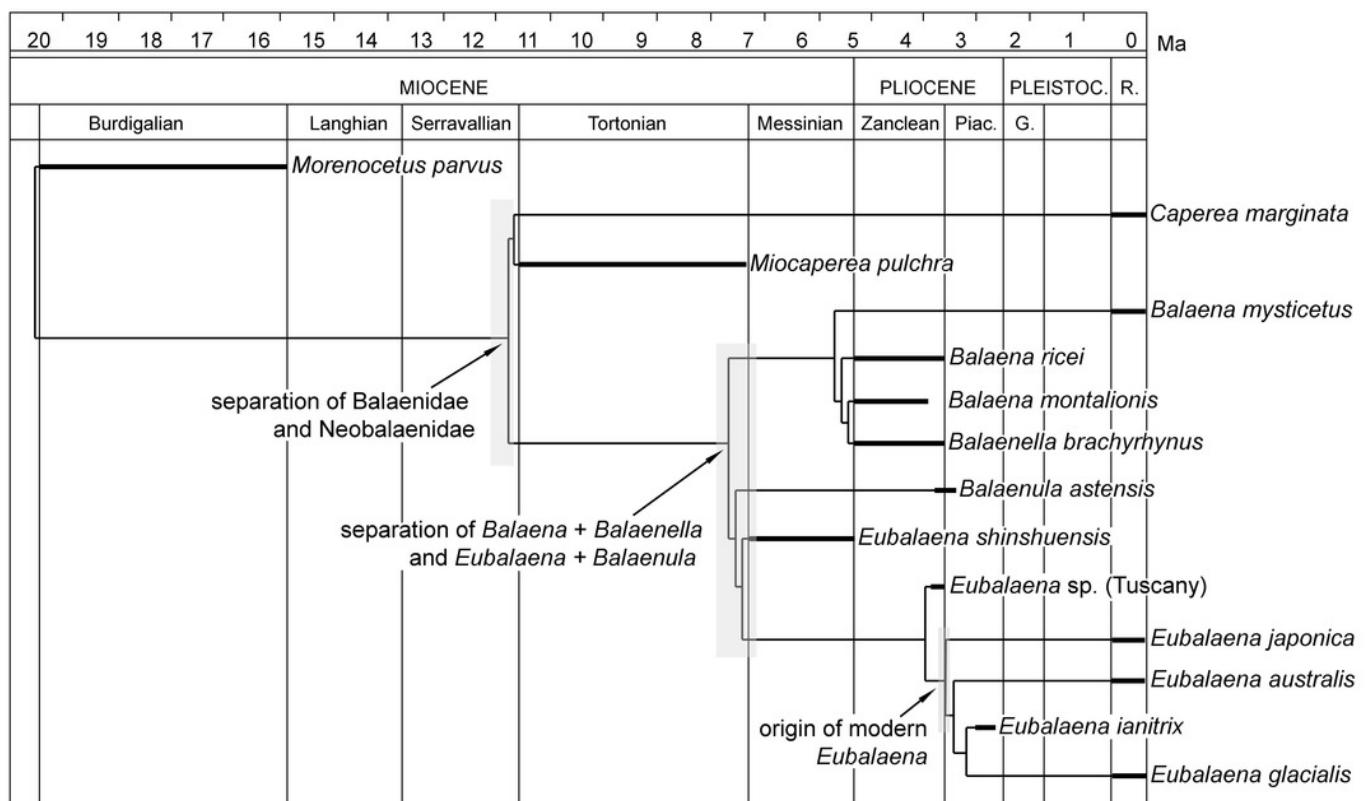
Measurements (in mm) of RBINS M. 880

Table 1 - Measurements (in mm) of RBINS M. 880 (cervical vertebrae complex, Balaenidae gen. et sp. indet.) and M. 2280 (left humerus, *Eubalaena* sp.). Characters are measured as preserved.

1 Table 1

2 Measurements (in mm) of RBINS M. 880 (cervical vertebrae) and M. 2280 (left humerus). Characters are

3 measured as preserved.

Character	Measure
M. 880 (cervical vertebrae)	
maximum anteroposterior length of whole complex	280
maximum transverse width of whole complex	423
maximum width across articular facets of atlas	384
maximum height of articular facets of atlas	175
posterior width of centrum of last cervical	246
posterior height of centrum of last cervical	201
M. 2280 (left humerus)	
total length	683
maximum proximal mediolateral width	355
maximum proximal anteroposterior width	458
anteroposterior diameter of humeral head	345
mediolateral diameter of humeral head	343
minimum mediolateral width of diaphysis	222
minimum anteroposterior width of diaphysis	271
distal mediolateral width	249
maximum distal anteroposterior width	364
anteroposterior length of radial facet	239
anteroposterior length of ulnar facet (including facet for olecranon)	250

Measurements (in mm) of the neurocranium RBINS M. 879a-f

Table 2 - Measurements (in mm) of the neurocranium RBINS M. 879a-f (holotype of *Eubalaena ianitrix* sp. nov.). Characters are measured as preserved.

1 **Table 2**

2 Measurements (in mm) of the neurocranium RBINS M. 879a-f (holotype of *Eubalaena ianitrix*

3 sp. nov.). Characters are measured as preserved.

Character	Measure
bizygomatic width	1660
estimated postorbital width	1760
width of occipital condyles	290
distance between lateral margins of exoccipitals	850
length of supraoccipital shield from foramen magnum to vertex	560
height between basicranium and vertex	71
transverse width of maxillae at vertex	290